DIFFERENT VIEWS AND APPROACHES IN HEALTH SCIENCES

EDITED BY
Assist. Prof. Dr. Müslüm TOPTAN
Spec. Dr. Zeliha AYHAN

AUTHORS
Prof. Dr. Yiğit UYANIKGİL
Prof. Dr. Mehmet TURGUT
Assoc. Prof. Dr. Servet ÇELİK
Assoc. Prof. Dr. Türker ÇAVUŞOĞLU
Assist. Prof. Dr. Bülent ÖZDEMİR
Assist. Prof. Dr. Fikret ALTINDAĞ
Spec. Dr. Aylin GÖKHAN
Op. Dr. Fevzi BIRIŞIK
Op. Dr. Yücel BILGIN
Res. Assist. Dr. Emel ÖZTÜRK
Res. Assist. Dr. Reyhan GÜNDÜZ
M.D. Akın ARSLAN
Res. Assist. Kubilay Doğan KILIÇ
Cansın ŞİRİN

İKSAD
Publishing House

DIFFERENT VIEWS AND APPROACHES IN HEALTH SCIENCES

EDITED BY

Assist. Prof. Dr. Müslüm TOPTAN

Spec. Dr. Zeliha AYHAN

AUTHORS

Prof. Dr. Yiğit UYANIKGİL
Prof. Dr. Mehmet TURGUT
Assoc. Prof. Dr. Servet ÇELİK
Assoc. Prof. Dr. Türker ÇAVUŞOĞLU
Assist. Prof. Dr. Bülent ÖZDEMİR
Assist. Prof. Dr. Fikret ALTINDAĞ
Spec. Dr. Aylin GÖKHAN
Op. Dr. Fevzi BIRIŞIK
Op. Dr. Yücel BILGIN
Res. Assist. Dr. Emel ÖZTÜRK
Res. Assist. Dr. Reyhan GÜNDÜZ
M.D. Akın ARSLAN
Res. Assist. Kubilay Doğan KILIÇ
Cansın ŞİRİN

İKSAD
Publishing House

(The Licence Number of Publicator: 2014/31220)
TURKEY TR: +90 342 606 06 75
USA: +1 631 685 0 853
E mail: iksadyayinevi@gmail.com
www.iksadyayinevi.com

It is responsibility of the author to abide by the publishing ethics rules.
Iksad Publications – 2021©

ISBN: 978-625-7636-85-8
Cover Design: İbrahim KAYA
May / 2021
Ankara / Turkey
Size = 16x24 cm

CONTENTS

PREFACE

Although there are different branches of medical school, physicians are always people-oriented and trying to find the most beneficial for people. Roads may cross in line with the same goal, it is necessary to act as a team, and a multidisciplinary approach gains importance. In this context, we wanted to gather the views of physicians working on different health science subjects under a single roof.

Editors

Assist. Prof. Dr. Müslüm TOPTAN[1]

Spec. Dr. Zeliha AYHAN[2]

[1] Harran Univesity , Faculty of Medıcıne
[2] Anesthesiology and Reanimation Specialist , Mehmet Akif İnan Research and Education Hospital.

CHAPTER 1

ORGAN PRESERVATION IN HEART TRANSPLANTATION: CURRENT SITUATION

Akın ARSLAN, M.D.[1]

[1] Sakarya University, Faculty of Medicine, Department of Cardiovascular Surgery, Sakarya, TURKEY. akinarslan@msn.com ORCID ID: 0000-0003-1380-6102

INTRODUCTION

With the proliferation of heart transplant centers and the increase in the distance to which the organ will be transferred, the organ's need for more extended protection has emerged. Providing this protection is very important in reducing mortality and morbidity. It is also essential to coordinate donor and recipient operations when planning this transfer process. To adjust the timing, the needs knowledge of whether the recipient has a previous mediastinal operations history. In this way, the ischemic period of the organ to be transplanted will be shorter.

1.1. PRESERVATION OF THE DONOR HEART

The critical process begins with the donor's heart being removed from the body after the initial arrest. The development of organ procurement possibilities from remote locations has brought the need to extend the extracorporeal period. Regardless of the distance and transfer method, the organ protection measures to be used should guarantee to minimize the damage. Otherwise, simultaneous operations (donor-recipient) will be at risk. Since a single method will be thought to be insufficient, various combinations have been tried. With the technique described by Shumway, the variety of hypothermia application (mechanical protection) and cold crystalloid cardioplegic solution (chemical protection) was determined as the ideal method to protect the heart.

1.1.1. Chemical Protection

1.1.1.1. Cardioplegia Solutions

The cardioplegia solution's main task is to arrest the heart in diastole as quickly as possible after the global ischemia period begins (after the cross-clamp is placed). With the interim doses given every 20-30 minutes for the cross-clamp duration, the arrest is maintained, while harmful metabolic products such as H + and lactate accumulated in the myocardium are washed away. The pH required for optimal metabolism is achieved by adding buffering agents such as bicarbonate, phosphate, or tri-hydroxy-methyl-amino methane (THAM) into the cardioplegic solution.

The upper limit of the generally accepted safe total ischemia time in heart transplant procedures is 3-4 hours. The ideal preservation solution should preserve the donor's heart's microvascular, cellular, and functional integrity during the ischemic period. For this reason, various solutions with proven efficacy have been produced. Cardioplegia solutions are classified according to the type of fluid they contain. These solutions are collected in two groups as blood and crystalloid cardioplegia. The crystalloid group is divided into two as intracellular and extracellular solutions.

1.1.1.1.1. Crystalloid Solutions

Experience with commonly used preservation solutions (University of Wisconsin and Celsior Solutions) has shown excellent myocardial function protection, especially when the ischemic time is less than 6 hours (Uesaka et al., 1999), (Boku et al., 2005). The University of

Wisconsin (UW) solution (CoStorSol® - Cold Storage Solution) is an "intracellular" based solution (low sodium, high potassium) and contains many impermeable molecules to minimize cellular swelling. Celsior solution, an "extracellular" solution, was developed due to the possibility of damaging effects of high potassium concentrations on the microvascular structure. In addition to many impermeable molecules (mannitol and lactobionate), Celsior contains glutamate, a substrate for energy production. It was also aimed to prevent oxygen-induced free radical damage (with reduced glutathione, histidine, and mannitol). Studies have shown that both solutions keep the donor heart under similar protection in terms of preservation (George et al., 2012). Crystalloid cardioplegic solutions contain specific electrolytes and do not contain organic matter such as blood or plasma. Other ready-to-use solutions Histidine-tryptophan-ketoglutarate (HTK) or Brettschneider's solution (Custodiol® solution), St. Thomas' Hospital cardioplegia solution (Plegisol®; Abbott Laboratories, Chicago, IL) belongs to this group. A long-term study reported that the Brettschneider's cardioplegia solution provided protective properties similar to cold blood cardioplegia (Sung et al., 2013). In another study, St. Thomas and HTK cardioplegia solutions were used together, resulting in similar survival rates to other methods (Lee et al., 2012). The del Nido crystalloid cardioplegia solution, which has been used in elective surgery for a long time, can also provide long protection in a single dose. In an animal experiment, del Nido and St. Thomas solutions are significant superiority to Custodiol cardioplegia solution have been reported (Karduz et al., 2020). In another study, an organ

care system that reduces ischemic time in long-distance organ transfers was tried, and the difference between Custodiol and blood cardioplegia was investigated. As a result, it has been stated that there is no clinically significant difference and can be safely preferred (Kaliyev et al., 2019).

1.1.1.1.2. Blood Cardioplegia

Melrose et al the use of hyperkalemic blood cardioplegia was described for the first time in 1955 (Melrose et al.,1955). It is obtained by mixing the patient's blood with the crystalloid cardioplegic solution taken from the extracorporeal circulation. The mixture is usually prepared by adding 2-4 or 8 units of blood against each crystalloid solution unit. The fact that blood is a physiological fluid and its ability to carry oxygen is a property believed in making it superior to other cardioplegic solutions. When blood cardioplegia is used, the heart is arrested in an oxygenated environment. Thus, the risk of staying hypoxic is minimized. A continuous oxygen supply is created with intermittent infusions during the arrest period. Thanks to the natural buffering systems in the blood, the risk of tissue acidosis is eliminated without the need to use other buffering agents. Due to its oncotic properties, the risk of interstitial edema is minimized after arrest caused by blood cardioplegia.

1.1.2. Mechanical Protection

1.1.2.1. Hypothermia

This method is based on the concept of hypothermia, and Bigelow (Bigelow et al., 1950) first introduced this concept to cardiac surgery

in 1950. Some positive changes occur in the heart with hypothermia. These are reduced myocardial metabolic rate and oxygen consumption, preventing cell death, and continuing electromechanical calm. However, some undesirable effects may occur due to hypothermia. In a hypothermic state, edema may develop in the myocardium (because the Na^+/K^+ pump is inactivated), the function and membrane stability of thrombocytes and leukocytes are impaired. According to the latest studies, it was found that the incidence of arrhythmias increased in the postoperative period with deep topical hypothermia, the incidence of injury to the phrenic nerve increased, and thermal damage to the epicardium (Efthimiou et al., 1991).

1.1.3. Operative Process

There are two essential steps in preventing myocardial damage during the operation. These are complete electromechanical arrest and a sufficient degree of hypothermia.

1.1.3.1. Cardioplegic Arrest

In this phase, the aim is to minimize myocardial ischemia while providing a motionless and bloodless operation area. The ideal has not been reached with any technique used today. Cardiac arrest is achieved by chemical means. It is generally based on solutions with high potassium concentrations. Cardioplegia solutions can be prepared as crystalloid or blood-based solutions depending on the circumstances. It can be administered antegrade (coronary arteries) or retrograde (coronary sinus) depending on the administration method. If given in the crystalloid form, the solution's temperature should be

cold at 4-10 °C, but if blood cardioplegia is used, it can be hypothermic or normothermic. For a period, crystalloid cardioplegia, which was famous for its ease of application, was gradually replaced by blood cardioplegia. A study compared classical cold blood cardioplegia with continuous warm reperfusion application with additional potassium and oxygenated blood infusion after the first arrest. The results were reported to be more positive (Pradas et al.,1996). Nowadays, there is a trend towards crystalloid-type solutions that provide long-term protection, especially del Nido. It is advantageous because it contains blood, oxygen, nutritional elements, buffer systems and contains free oxygen radical scavenging agents. However, nowadays, discussions continue about the application methods of blood cardioplegia. For example, retrograde or anterograde, normothermic or hypothermic administration of blood cardioplegia can be mentioned. With time, significant changes have occurred in the content of a cardioplegic solution.

Cardioplegia means the controlled arrest of the heart. Until today, substances such as potassium, magnesium, procaine, low-density calcium have been used as arresting agents in cardioplegic solutions. They are potassium solutions that are widely used today. Cardioplegic solutions stop the heart by depolarizing the cell membrane. When a complete electromechanical silence is achieved, the heart's oxygen requirement drops to 0.3 ml per minute per 100 grams of myocardial tissue at 20 °C. When the myocardial temperature is reduced to 10 °C, the oxygen demand drops to 0.15 ml/100 grams/minute. If it is considered that the oxygen requirement of the working or fibrillated

heart is 2-3 ml/100 gm/min and it increases up to 5-6 ml/100 gm/min in the heart whose energy stores are depleted, it is better. It is understood how vital arrest created with cardioplegic solutions is in myocardial protection.

1.1.3.1.1. Antegrade Cardioplegic Cardiac Arrest

It is applied directly from the aortic root or coronary ostia. The coronary perfusion rate is set as 150 ml/min/m^2. In pediatric doses, a dose calculation of 50 ml/kg can also be used. For antegrade administration, the cardioplegic solution is delivered with a perfusion pressure of 70 mmHg.

1.1.3.1.2. Retrograde Cardioplegic Cardiac Arrest

Although useful as antegrade arrest, the middle part of the right ventricle and the right atrium is less perfused. This method is more effective in coronary artery occlusions in elective cases. The best approach is to deliver directly from the coronary sinus. Perfusion pressure should not exceed 50 mmHg. Retrograde perfusion was first applied by Pratt and later by Lillehei (Lillehei et al., 1956). Cleaning of the various embolism accumulated in the coronary system by applying retrograde perfusion is a significant advantage.

1.1.3.1.3. Pharmacological Protection Supports

Glucose-Insulin-Potassium Solution: Sodi-Pollares used it for the first time in 1965 in acute myocardial infarction and detected electrocardiographic improvements in these patients (Sodi-Pollares, 1982). The purpose of this solution is to increase the amount of

glycogen in the myocardium. It has been shown that administration of glucose-insulin-potassium starting 12 hours before the operation increases myocardial glycogen content.

Glutamate-aspartate solutions: The inclusion of Krebs cycle intermediates such as Glutamate and Aspartate in cardioplegic solution has been shown to have clinical benefit. This type of solution was used only in patients who had isolated coronary surgery. Similarly, Rosenkranz et al. Recommend glutamate-containing blood cardioplegia in patients with cardiogenic shock (Rosenkranzet al., 1983).

Calcium channel blockers: Calcium is the critical electrolyte of ischemia and reperfusion injury. During ischemia, calcium accumulates inside the cell. This occurs as a result of the loss of cell membrane integrity. The reason is that the ATP-dependent Na^{+}/Ca^{++} active pump cannot fulfill its function due to the lack of energy, and the calcium entering into the cell by diffusion cannot be expelled. The accumulated calcium degrades high energy phosphates and causes energy loss by spending energy on active pumps. ATPase disrupts cell integrity by activating proteases and phospholipases. Calcium channel blockers block slow calcium channels. Thus, they prevent the initial intracellular calcium accumulation. Reducing the myocardial workload and therefore energy consumption by lowering afterload protects the myocardium with an indirect effect.

Xanthine oxidase inhibitors: Xanthine is formed from hypoxanthine under xanthine oxidase catalysis. Meanwhile, toxic radicals are

released into the environment. Although the presence of xanthine oxidase enzyme in the human heart is doubtful, the use of xanthine oxidase inhibitor allopurinol has been shown to reduce the risk of myocardial damage in two clinical studies (Hopson et al., 1995).

Vitamins E and C: The antioxidant and cytoprotective properties of both vitamins are known. The study results report that the no-reflow phenomenon, which is observed in approximately one-third of the patients after acute myocardial infarction and after percutaneous coronary intervention, increases significantly in the case of depletion of antioxidants (Matsumoto et al., 2004).

Nucleoside transport inhibition: Nucleosides are ATP degradation products. Adenosine is formed as a result of ATP breakdown during ischemia. 5'-nucleotidases form adenosine. The adenosine formed is carried up to the endothelial cell by nucleoside transporters. It is broken down into inosine and hypoxanthine by adenosine deaminase in the endothelial cell. Usually, adenosine, inosine, and hypoxanthine form a nucleoside pool and are used in ATP synthesis when needed. During bypass, the nucleoside pool elements in endothelial cells pass into the vessel lumen and are washed with the cardioplegic solution and non-coronary collateral flow. Adenosine transport to the endothelium should be prevented by drugs such as lidoflazine, myoflazine, and soluflazine, which are nucleoside transport inhibitors.

Iron binders: While free oxygen radicals are formed, more harmful hydroxyl radicals can be formed from the superoxide anion, which can

be considered partially innocent, under the catalysis of Fe^{++}. This reaction can be prevented if desferrioxamine is bound with iron.

Carnitine: In the ischemic environment, myocytes use carbohydrates as the main metabolic product. Fatty acids accumulate within the cell. Carnitine enables the fatty acid derivatives accumulated in the cell to be transported into the mitochondria. Thus, it creates an alternative energy source for the cell.

1.1.3.2. Hypothermic Circulatory Arrest

The hypothermic circulatory arrest is rarely used in transplant surgery, but it is a life-saving technique when necessary. A study reported that this situation has no adverse effect on the postoperative process Sorabella et al 2016.

1.1.3.3. Reperfusion

It was shown in the study that the aerobic metabolism of the myocardium was improved, and diastolic compliance was increased by applying hot blood cardioplegia (hot shot) before the cross-clamp was lifted (Teoh et al., 1986).

CONCLUSION

For many years, intensive efforts have been shown to protect heart tissue from ischemic damage and provide ideal conditions. The aim is to deliver the organ transplanted to the target with minimal risk in the extracorporeal environment. In today's needs, long surgical modalities can be performed with a single dose of cardioplegia. However, some surgical teams aim to keep the result in maximum benefit with

additional protection measures. Considering that heart transplants have become widespread in the pediatric population and this rate will gradually increase, it is inevitable that the preservation of the immature myocardium will require additional features. Moreover, if there are accompanying non-cardiac anomalies in these cases, the importance of long-term full protection will be even more critical. Therefore, clinical studies, including large series, including animal experiments, should increase and are valuable.

REFERENCES

Bigelow Wg, Callaghan Jc, Hopps Ja. General Hypothermia For Experimental Intracardiac Surgery; The Use Of Electrophrenic Respirations, An Artificial Pacemaker For Cardiac Standstill, And Radio-Frequency Rewarming İn General Hypothermia. Trans Meet Am Surg Assoc Am Surg Assoc. 1950; 68:211-9.

Boku, N., Tanoue, Y., Kajihara, N., Eto, M., Masuda, M., & Morita, S. (2006). A Comparative Study of Cardiac Preservation with Celsior or University of Wisconsin Solution with or without Prior Administration of Cardioplegia. The Journal of Heart and Lung Transplantation, 25(2), 219–225. doi:10.1016/j.healun.2005.08.009

Efthimiou J, Butler J, Woodham C, Benson MK, Westaby S. Diaphragm paralysis following cardiac surgery: role of phrenic nerve cold injury. Ann Thorac Surg. 1991 Oct;52(4):1005-8.

Hopson SB, Lust RM, Sun YS, Zeri RS, Morrison RF, Otaki M, Chitwood WR Jr. Allopurinol improves myocardial reperfusion injury in a xanthine oxidase-free model. J Natl Med Assoc. 1995 Jul;87(7):480-4.

J George TJ, Arnaoutakis GJ, Beaty CA, Shah AS, Conte JV, Halushka MK. A novel method of measuring cardiac preservation injury demonstrates University of Wisconsin solution is associated with less ischemic necrosis than Celsior in early cardiac allograft biopsy specimens. George TJ, Arnaoutakis GJ, Beaty CA, Shah AS, Conte JV, Halushka MK. Heart Lung Transplant. 2012 Apr;31(4):410-8. doi: 10.1016/j.healun.2011.11.023. Epub 2011 Dec 30.

Kaliyev R, Lesbekov T, Bekbossynov S, Bekbossynova M, Nurmykhametova Z, Novikova S, Smagulov N, Medressova A, Faizov L, Ashyrov Z, la Fleur P, Samalavicius R, Pya Y. Comparison of Custodiol vs warm blood cardioplegia and conditioning of donor hearts during transportation with the organ care system. J Card Surg. 2019 Oct;34(10):969-975. doi:

10.1111/jocs.14162. Epub 2019 Jul 23. PMID: 31332833; PMCID: PMC6852406.

Karduz G, Yaman MO, Altan M, Sahin G, Toraman F, Aksu U. St. Thomas and del Nido cardioplegia are superior to Custodiol cardioplegia in a rat model of donor heart. Scand Cardiovasc J. 2020 Nov 13:1-7. doi: 10.1080/14017431.2020.1846772. Epub ahead of print. PMID: 33185130.

Lee KC, Chang CY, Chuang YC, Sue SH, Yang HS, Weng CF, Lee YT, Huang WS, Chen IC, Wei J. Combined St. Thomas and histidine-tryptophan-ketoglutarat solutions for myocardial preservation in heart transplantation patients. Transplant Proc. 2012 May;44(4):886-9. doi: 10.1016/j.transproceed.2011.11.010. PMID: 22564575.

Lillehei Cw, Dewall Ra, Gott Vl, Varco Rl. The Direct Vision Correction Of Calcific Aortic Stenosis By Means Of A Pump-Oxygenator And Retrograde Coronary Sinus Perfusion. Dis Chest. 1956 Aug;30(2):123-32.

Matsumoto H, Inoue N, Takaoka H, Hata K, Shinke T,Yoshikawa R, Masai H, Watanabe S, Ozawa T,Yokoyama M. Clin. Depletion of antioxidants is associated with…. no-reflow phenomenon in acute myocardial infarction. Cardiol. 2004 Aug;27(8):466-70.

Melrose Dg, Dreyer B, Bentall Hh, Baker Jb. Lancet. Elective Cardiac Arrest. 1955 Jul 2;269(6879):21-2.

Pradas, Gonzalo & Cuenca, Jose & Juffe stein, Alberto. Continuous warm reperfusion during heart transplantation. The Journal of thoracic and cardiovascular surgery (1996).111.784-90. 10.1016/S0022-5223(96)70338-0.

Rosenkranz ER, Buckberg GD, Laks H, Mulder DG. Warm induction of cardioplegia with glutamate-enriched blood in coronary patients with cardiogenic shock who are dependent on inotropic drugs and intra-aortic balloon support. J Thorac Cardiovasc Surg. 1983 Oct;86(4):507-18.

Sodi-Pollares D. Theoretical effect in human heart disease of low-sodium high-potassium diet therapy on intracellular adsorbed sodium and potassium. Physiol Chem Phys. 1982;14(5):439-43

Sorabella, R. A., Guglielmetti, L., Bader, A., Gomez, A., Takeda, K., Chai, P. J., Takayama, H., Bacha, E. A., Naka, Y., & George, I. (2016). The Use of Hypothermic Circulatory Arrest During Heart Transplantation Does Not Worsen Posttransplant Survival. The Annals of thoracic surgery, 102(4), 1260–1265. https://doi.org/10.1016/j.athoracsur.2016.03.058

Sung SY, Lin CY, Song JY, Tsai YT, Kao CH, Lee CY, Lin YC, Hsu PS, Tsai CS. Myocardial protection in donor heart preservation: a comparison between Bretschneider's histidine-tryptophan-ketoglutarate solution and cold blood cardioplegia. Transplant Proc. 2014 May;46(4):1077-81. doi: 10.1016/j.transproceed.2013.11.056. PMID: 24815133.

Teoh KH, Christakis GT, Weisel RD, Fremes SE, Mickle DA, Romaschin AD, Harding RS, Ivanov J, Madonik MM, Ross IM, et al. Accelerated myocardial metabolic recovery with terminal warm blood cardioplegia. J Thorac Cardiovasc Surg. 1986 Jun;91(6):888-95.

Uesaka T, Chiba Y, Ihaya A, Nara M, Niwa H, Muraoka R. Low-potassium University of Wisconsin solution for cardioplegia: improved protection of the isolated ischemic neonatal rabbit heart. Cardiovasc Surg. 1999 Dec;7(7):723-9.

CHAPTER 2

STEREOLOGICAL METHODS USED IN THE HISTOMORPHOMETRIC INVESTIGATIONS OF THE TESTIS

Assist. Prof. Dr. Fikret ALTINDAĞ [1]

[1] Department of Histology and Embryology, Medical, Van, Turkey.
altindagfikret@gmail.com.tr.ORCID ID : 0000-0002-4074-5168

INTRODUCTION

The histomorphometric structure of the testis can change depending on some biological, developmental, and pathological conditions. These changes can directly result in changes in the reproductive system. Testicular histology plays an important role in explaining pathological and physiological changes in both humans and experimental studies. Histopathological evaluations and semi-quantitative evaluations are quite insufficient in examining the morphological structure of the tissue with terms such as hyperplasia, hypoplasia, hypertrophy, and atrophy. Thus, it is important to apply quantitative methods in which possible histopathological changes in the tissue can be determined by statistically comparing more detailed and obtainable numerical data in the examination of the testis. Stereological examination methods include unbiased counting and calculation methods used in calculating the numerical values of all structures that make up the testis. By applying stereological examination methods, parameters such as the total volume of the testis, total spermatogenic cells, the total number of Sertoli and Leydig cells, total seminiferous tubule length and diameter, total interstitial area volume in testis and thickness of tunica albuginea layer can be calculated with numerical values.

In this study, it is presented the unbiased stereological methods used in the determination of the histomorphometric and physiological changes that may occur in the testis in humans and experimental studies.

1. STEREOLOGY

Stereology is a branch of science that reveals the 3-dimensional properties of tissue such as volume, cell number, surface area, vessel, and tubule length from 2-dimensional sections taken from tissues. By now, many methods have been used to investigate the histomorphometric properties of the tissue. Each method used has more or less some error sources. New methods have been developed to resolve the error sources of the methods used. However, among these methods, the most reliable and most interesting method was stereological methods (Ünal ve ark., 2002).

Stereological methods are frequently used in fields such as medicine, astronomy, geology, mathematics, and engineering. The most important feature of stereological methods is to reduce the workload and loss of time, allowing to obtain unbiased and reliable mathematical data with statistical accuracy (Gundersen, 1987; Mayhew, 2006).

1.1. Stereological Examination of the Testis

Testicular quantitative data obtained as a result of stereological methods are very important in determining the structural and functional characteristics of the testis. Structural parameters such as the total number of cells, the length, and diameter of the seminiferous tubules, total connective tissue volume in the testis that can be determined by stereological methods are widely used in toxicology, pathology, physiology, and testicular infertility. Quantitative data of testis morphology are needed to investigate the ultrastructural changes

associated with the processes of the therapeutic conditions in the testis. These data are also very important in the investigation of testicular biopsy and fertilization. Because stereological data are more accurate, precise, reliable, and effective than data obtained from two-dimensional morphometric examinations. Accuracy is a measurement of how close that a made measurement is to the truth or true value. Precision is a measurement of how close that a made measurements are to each other (Noorafshan, 2014).

Instead of examining the whole tissue in stereological studies of the testis, the tissue is systematically examined by random sampling through various geometric probes. Thus, by reducing the workload, more efficient and effective results are obtained (Gundersen, 1986; Gundersen ve ark., 1988). Accurate biological data obtained by stereological methods make it possible to evaluate the extent of pathological conditions such as testicular atrophy, hypertrophy, hypotrophy, hyperplasia, and hypoplasia (Noorafshan, 2014).

The most effective way to refrain prejudice and acquire correct data in the studies planned to be carried out in the testis is to apply a meticulous experimental model. For this, each stage of the experiment, from the fixation stage of the tissue to the sampling and microscopic examination, should be done according to the determined standard rules. While modeling an accurate, efficient, and effective study, the number of sampling at each sampling stage, such as tissue fragments, section, area, measurement, can be reduced without reducing the degree of accuracy to obtain precise estimates

(Mandarim-de-Lacerda, 2003; Altindağ ve Rağbetli, 2021; Noorafshan, 2014). To provide this, numerical values of the formulated study such as error coefficient error (CE) and coefficient of variation (CV) can be used. The CE is calculated to obtain the optimum number of sections, while the CV is calculated to obtain the optimum number of experimental animals in each group (Sonmez et all., 2010).

1.2. Orientator Method

Isotropic cross-sections are needed to evaluate parameters such as length and surface area in three-dimensional structures. The most common methods used to obtain isotropic uniform random sections (IURS) are orientator and isector methods. Isotropic uniform random sectioning means that the cut direction and position cannot be predicted, indicating that it is random in three-dimensional structure (Mattfeldt et all., 1990; Nyengaard and Gundersen, 1992; Noorafshan, 2014).

The testis is placed on a circle that is evenly divided and numbered from 1 to 10. A random number is chosen and the testicle is cut in half with a sharp knife according to the chosen number. The cut testis piece is divided into parallel sections by placing it on a circle numbered with numbers 0-9 and divided at equal intervals. These parts are embedded in paraffin (Mattfeldt et all., 1990; Noorafshan, 2014; Altindağ and Özdek, 2021).

1.3. Calculation of Total Testicular Volüme

The volume of testicular tissue is calculated by the Cavalieri principle. Here, the testis tissue is divided into slices or sections parallel to each other at equal intervals from the beginning to the end. The areas of the surfaces facing the same side of each slice or section obtained using the dotted area measuring ruler are calculated. The total number of points coinciding on tissue is calculated and the area of the slice or cross-section is calculated by multiplying the area covered by a point. The total volume of the testis is calculated by multiplying the total surface area obtained from all slices or sections by the thickness of the slice or section. It can formulate the testicular volume calculation as follows:

$V_{ref} = \Sigma P \times a(p) \times t$

V_{ref}; the total or reference volume of the testis, ΣP; the total number of points in the section or slices, a (p); the area covered by a point, t; shows the thickness of section or slice (Canan ve ark., 2002; Altindağ and Özdek, 2021)

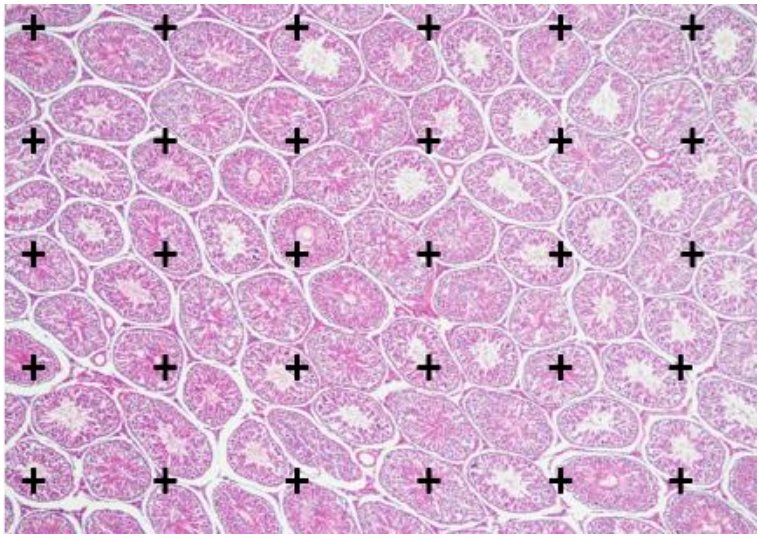

Figure 1: Application of the dotted area measuring grid to testicular tissue

1.4. Calculation Of Volume Of The Seminiferous Tubule, Germinal Epithelium, And Interstitial Tissue

Using the dotted area measuring grid used in testicular volume calculation, the corresponding points on the seminiferous tubule, germinal epithelium, and interstitial tissue can be collected and multiplied by the area covered by a point and the section thickness, thus the volumes of the structures can be calculated. The volume density of each of these structures is calculated by the formula below (Gundersen, 1986; Noorafshan, 2014; Altindağ and Özdek, 2021).

$$Vv(\text{structure}) = \frac{\sum P(\text{structure})}{\sum P(\text{total})}$$

$Vv_{(structure)}$: The volume density of the relevant structure, $\sum P_{(structure)}$: The total number of points on the relevant structure, $\sum P_{(total)}$: The total number of points corresponding to the testicular tissue

1.5. Calculation Of The Total Number And Numerical Density Of Cells İn The Testis

The physical dissector counting method is used to calculate the total number and numerical density of cells in the testis. For this, consecutive sections are taken. Cells observed in the first section but not observed in the consecutive section are included in the count in the area limited by an unbiased counting frame (dissector probe) in the sections. While applying the physical dissector method, area sampling is done. Cell counts are made on all sampled areas. The total dissector volume (ΣV_{dis}) is calculated by multiplying the volume of the counting frame used to calculate the cell number by the total number of counting frames. The numerical density of the cell is calculated by dividing the total dissector particles (cells) (ΣQ^-) counted in the total dissector volume by the total dissector volume (Ünal ve ark., 2002; Altindağ and Özdek, 2021).

This can be formulated as follows:

$N_V = \Sigma Q^- / \Sigma V_{dis}$

N_V: Numerical density of cells

ΣQ^-: Total number of dissector cells

ΣV_{dis}: Total dissector volume

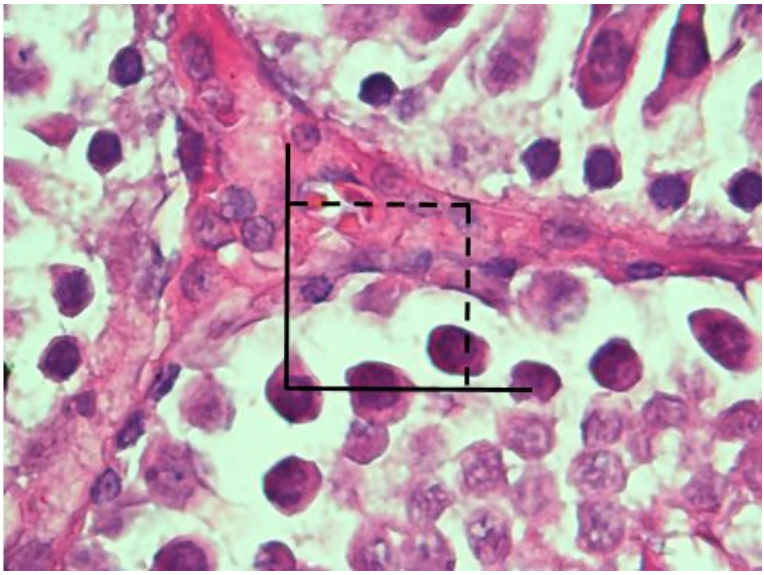

Figure 2: Applying unbiased count frame to testicular tissue for cell counting

1.6. Calculation Of The Length Density And Total Length Of Seminiferous Tubule

The unbiased counting frame is used to calculate the tubule length density and total length. The right and lower edges of this frame are considered prohibited edges. Seminiferous tubules touching these edges are not included in the count. If all or part of the tubule falls within the counting frame but not touching the prohibited edges are counted. The following formula is used for the seminiferous tubule length density;

$$\mathrm{Lv(structure)} = 2.\frac{\sum Q}{\sum P \text{ x } a/ç}$$

$L_{V(structure/ref)}$: The length density of seminiferous tubule

∑Q: The number of tubule profiles corresponding to the counting zone of the counting frame

∑P: Total number of count frame

a/ç: Area of a counting frame

The total seminiferous tubule length is calculated by multiplying the seminiferous tubule length density found as a result of the calculation by the total testicular volüme (Gundersen, 1986; Noorafshan, 2014; Altindağ and Özdek, 2021).

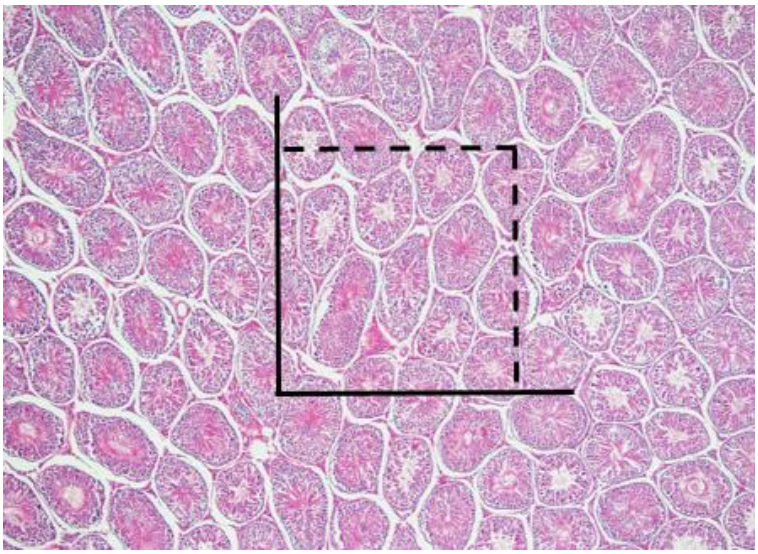

Figure 3: Applying unbiased count frame to testicular tissue to calculate tubule length density

1.7. Calculation Of Surface Area Density Of Seminiferous Tubule

Line grids are used to calculate the density of the seminiferous tubule surface area, each associated with a point. Line grids are placed on the

images of testicular tissue. The total number of points where the luminal surface of the seminiferous epithelium and the grid intersect, the total number of grids corresponding to the reference area, and the length of a grid are calculated. The surface area density of the seminiferous tubule is calculated by substituting the obtained values in the formula (Gundersen, 1986; Noorafshan, 2014; Altindağ and Özdek, 2021).

The following formula is used for this;

$$Sv(epitel/ref) = 2.\frac{\sum K}{\sum P \text{ x } k/p}$$

S_V: The surface area density of seminiferous tubule

$\sum K$: The total number of points where the luminal surface of the seminiferous epithelium and the grid intersect

$\sum P$: Total number of grids corresponding to the reference area

k/p: Length of a grid

1.8. Calculation Of The Epithelium Height Of The Seminiferous Tubules

To calculate the height of the seminiferous tubule epithelium, the volume density and tubule surface area density of the seminiferous tubule epithelium must first be calculated. The volume density of the seminiferous tubule epithelium is calculated with a dotted area measuring ruler. The volume density (Vv) of the seminiferous tubule epithelium is calculated by dividing the total number of points corresponding to the tubular epithelium in the area measurement scale

used, by the number of points corresponding to the all reference area (Gundersen, 1986; Noorafshan, 2014; Altindağ and Özdek, 2021).

The following formula is used to calculate the epithelium height of the seminiferous tubule;

$$Eh = \frac{Vv\ (epitel/ref)}{Sv\ (epitel/ref)}$$

E_h: The epithelium height of the seminiferous tubule

V_v: The epithelium volume density of the seminiferous tubule

S_v: The surface area density of seminiferous tubule

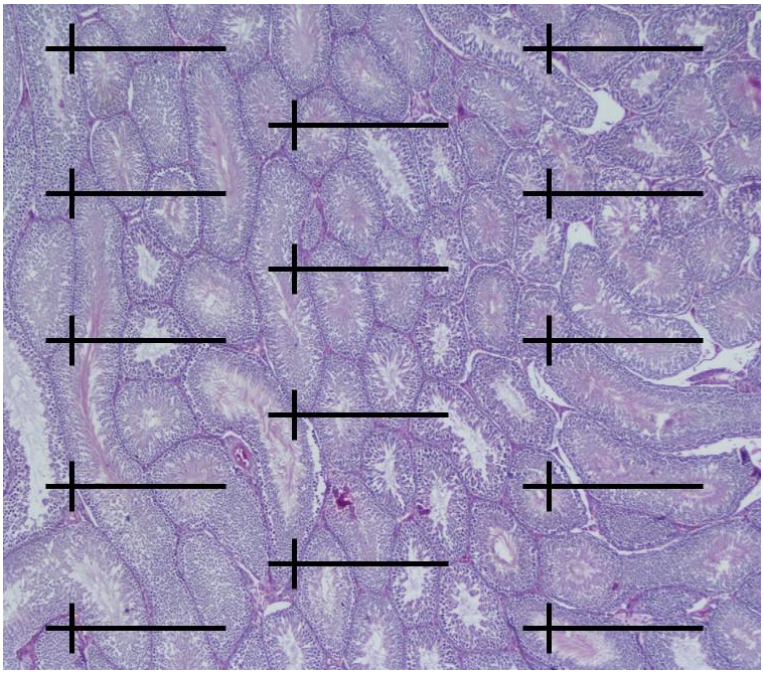

Figure 4: The superimposed of a grid of test lines on the image of the section.

REFERENCES

Altindağ, F., Özdek, U. (2021). Protective Eff ects of Chitosan and Chitosan Oligosaccharide on Sodium Fluoride-Induced Testicular Damage in Male Rats: A Stereological and Histopathological Study. Kafkas Univ Vet Fak Derg, 27, 183-189.

Altindağ, F., Rağbetli, M. Ç. (2021). The effect of maternal treatment with diclofenac sodium and thymoquinone on testicular parameters in rat offspring. Revista Internacional de Andrología, 19, 34-40.

Canan, S., Şahin, B., Odacı, E., Ünal, B., Aslan, H., Bilgiç, S., Kaplan, S. (2002).

Toplam Hacim, Hacim Yoğunluğu ve Hacim Oranlarının Hesaplanmasında Kullanılan Bir Stereolojik Yöntem: Cavalieri Prensibi. T Klin Tıp Bilimleri, 22, 7-14.

Gundersen, H. J. G. (1986). Stereology of arbitrary particles. A review of unbiased number and size estimators and the presentation of some new ones, in memory of William R. Thompson. J. Microsc, 143, 3–45.

Gundersen, H.J.G., Jensen EB (1987). The efficiency of systematic sampling in and its prediction. J Microsc, 147, 3, 229-263.

Gundersen, H. J. G., Bagger, P., Bendtsen, T. F., Evans, S. M., Korbo, L., Marcussen, N., Moller, A., Nielsen, K., Nyengaard, J. R., Pakkenberg, B., Sorensen, F. B., Vesterby A., West, M, J. (1988). The new stereological tools: Disector, fractionator, nucleator and point sampled intercepts and their use in pathological research and diagnosis. APMIS, 96, 857-881.

Mandarim-de-Lacerda, C. A. (2003). Stereological tools in biomedical research. An.Acad. Bras. Cienc, 75, 469–486.

Mattfeldt, T., Mall, G., Gharehbaghi, H., Möller, P., 1990. Estimation of surface area and length with the orientator. J. Microsc, 159, 301–317.

Mayhew, T. M. (2006). Stereology and the placenta: Where's the Point? A Review. Placenta, 27, 17-25.

Noorafshan, A. (2014). Stereology as a valuable tool in the toolbox of testicular research. Annals of Anatomy, 196, 57-66.

Nyengaard, J. R., Gundersen, H. J. G. (1992). The isector: a simple and direct method for generating isotropic, uniform random sections from small specimens. J. Microsc, 165, 427–431.

Sönmez, O. F., Odaci, R., Bas, O., Kaplan, S. (2010). Purkinje cell number decreases in the adult female rat cerebellum following exposure to 900 MHz electromagnetic field. Brain Research, 1356; 95-101.

Ünal, B., Aslan, H., Canan, S., Şahin, B., Kaplan, S. (2002). Biyolojik Ortamlardaki Objelerin Sayımı Yapılırken Kullanılan Eski (taraflı) Metotların Önemli Hata Kaynakları ve Çözüm Önerileri. T Klin Tıp Bilimleri, 22, 1-6.

CHAPTER 3

RESOLVING EMBRYOLOGICAL AND HISTOLOGICAL DEPICTIONS OF CHOROID PLEXUS

Aylin GÖKHAN[1] Spec. Dr.,
Res. Assist. Kubilay Doğan KILIÇ[2] ,Cansın ŞİRİN[3] ,
Assoc. Prof. Dr. Türker ÇAVUŞOĞLU[4] ,
Assoc. Prof. Dr. Servet ÇELİK[5] , Prof. Dr. Yiğit UYANIKGİL[6] ,
Prof. Dr. Mehmet TURGUT[7]

[1] Ege University School of Medicine, Department of Histology and Embryology, Izmir, Turkey, aylin.gokhan@ege.edu.tr, 0000-0002-6254-157X
[2] Ege University School of Medicine, Department of Histology and Embryology, Izmir, Turkey, kubilay.dogan.kilic@ege.edu.tr, 0000-0002-9484-0777
[3] Ege University School of Medicine, Department of Histology and Embryology, Izmir, Turkey, cansinsirin@gmail.com, 0000-0002-4530-701X
[4] Ege University School of Medicine, Department of Histology and Embryology, Izmir, Turkey, turker.cavusoglu@ege.edu.tr, 0000-0001-2345-6789
[5] Ege University School of Medicine, Department of Anatomy, Izmir, Turkey, servet.celik@ege.edu.tr, 0000-0002-1102-4417
[6] Ege University School of Medicine, Department of Histology and Embryology, Izmir, Turkey, yigit.uyanikgil@ege.edu.tr, 0000-0002-4016-0522
[7] Adnan Menderes University School of Medicine, Department of Neurosurgery, , Aydın, Turkey, drmturgut@yahoo.com, 0000-0001-7130-2530

INTRODUCTION

The embryonic period, also known as organogenesis or embryogenesis, begins at the third week of development and continues to the end of the eighth week. At the beginning of the third week, CNS is seen, and the brain, forming from the neural tube, expands into three primary brain vesicles, that is, the forebrain, the midbrain, and the hindbrain, also known as, prosencephalon, mesencephalon, and rhombencephalon, respectively, during the third and fourth weeks of development. By the fifth week, the primary brain vesicles are subdivided into five secondary vesicles that will thereafter establish different parts of the cranial architectures, including CPx.

1. BRAIN VENTRICLES

The prosencephalon is divided into the telencephalon (future cerebral hemispheres) and diencephalon (future optic cup and stalk, thalamus, hypothalamus, and epiphysis); the mesencephalon remains the same name and contributes to anterior/visual and posterior/auditory colliculi; and the rhombencephalon is evolved into two secondary brain vesicles, the metencephalon (future pons and cerebellum) and the myelencephalon (future bulb also known as medulla oblongata). The central canal of the spinal cord is continuous with the related vesicles (Moore, Persaudi and Torchia, 2016).

The walls and cavities of brain vesicles expand and form the adult brain structures such as the ventricular system. The paired lateral ventricles, right and left, are derived from the cavities of the telencephalic vesicles which also form the rostral part of the third

ventricle; even though it is widely derived from the cavity of the diencephalon. The cavity of the midbrain give rise to the aqueduct in the mesencephalon known as the cerebral aqueduct, and in addition, the hindbrain (rhombencephalon) engenders the fourth ventricle (Friedrich and Jens, 2018; Felten, O´banion and Maida, 2015).

After the right and left lateral ventricles assume a C-shaped structure and are connected with the third ventricle via the interventricular foramen (foramen of Monro), the connection between the third and fourth ventricles is established through a narrow lumen, known as the aqueduct of midbrain (aqueduct of Sylvius). While the diamond-shaped fourth ventricle extends inferiorly into the central canal of the spinal cord, the lateral openings – lateral aperture (foramen of Luschka) of the fourth ventricle and median opening – median aperture (foramen of Magendie) of fourth ventricle allow the cerebrospinal fluid (CSF) to flow from the inner to the outer subarachnoid spaces (into cisterns) which are projected between the arachnoid and the pia mater (Moore et al. 2016; Sadler, 2014).

The arterial blood supply system of the CPx is as follows: arterial vessels of the lateral ventricle are supplied by the anterior choroidal artery (from the internal carotid artery) and the lateral posterior choroidal branch of the posterior cerebral artery; those of the third ventricle are fed by the medial posterior choroidal branch of the posterior cerebral artery; those of the fourth ventricle are supplied by the posterior inferior cerebellar artery (from the vertebral artery) and

the anterior inferior cerebellar artery (from the basilar artery) (Friedrich and Jens, 2018; Gupta, 2017).

2. CHROID PLEXUS

CPx develops from several locations as follows (Catala, 2019; Ghersi-Egea, Strazielle, Catala, Silva-Vargas, Doetsch and Engelhardt, 2018).

(i) The hindbrain CPx of the fourth ventricle is the first to appear.

(ii) Then, the telencephalic CPx is developed in each lateral ventricle.

(iii) Finally, the diencephalic CPx of the third ventricle develops.

The wall of the closed neural tube is formed by neuroepithelial cells, which rapidly divide and produce a thick pseudostratified epithelium with functional complexes, called neuroepithelium, that gives rise to the epithelial part of CPx. These single ependymal cells layer with the underlying vascular mesenchyme form the main structure of the CPx in the lateral ventricles as well as third and fourth ventricles. The thin ependymal layer supported with the overlying pia mater is known as choroid membrane. The vascular mesenchyme actively proliferates and thus forms CPx from sac-like invaginations through the ventricular cavities and CPx secretes CSF into the entire ventricular area (Kierszenbaum and Tres, 2015; Pawlina and Ross, 2018) Figures 1, 2, and 3 provide illustrations along with photomicrographs of the main structure of CPx. (Figures 1, 2 and 3)

In 1975, Netsky and Shuangshoti well demonstrated the developmental morphology of the brain ventricles in association with the CPx (Netsky and Shuangshoti, 1975). Many researchers have also been interested in staging the development of the CPx. Human CPx maturation period based on histological alterations is divided into four stages starting at the seventh week of development according to different studies (Table 1) (Dziegielewska, Ek, Habgood and Saunders, 2001; Kaur, Rathnasamy and Ling, 2016; Liddelow, 2015; Lun, Monuki and Lehtinen, 2015). The first stage starts at the seventh week: CPx encompasses the ventricles and has a highly pseudostratified epithelium without distinctive villi; the nuclei are located in a central position and do not contain glycogen. The second stage starts at the ninth week: the size of CPx is larger than the ventricles; the epithelium is villous and appears in the form of short columns. The third stage starts at the 17th week: CPx is larger than the ventricles but not as in the second stage; the nuclei are centrally or apically located; glycogen content in the cells is moderate. The fourth stage begins in the nineteenth week: CPx is small compared to the ventricles; the epithelium is squamous with centrally or basally located nuclei; glycogen is not observed.

2.1. Cellular Characteristics of the Choroid Plexus

CPx is formed by cuboidal epithelial cells which are highly polarized. These cells have microvilli and their apical domain contains tight junctions that connect adjacent cells to structure the blood-CSF barrier. Tight junctions' markers are as follows: claudins 1-3, and 11,

ZO 1-3, and occludin. In addition, transthyretin protein, synthesized by the liver, and also the CPx, can be used as tumor marker (Kovacs, 2018).

The choroidal epithelial cells, rich in mitochondria that supply the required energy necessary for high metabolic turnover, rest on the basal lamina with interdigitating folds at the basolateral domain. Fenestrated capillary endothelial cells that lack tight junctions permit the net flow of water, solutes, and proteins to enter the surrounding stroma; however, these molecules cannot pass directly into the CSF because of the limitation of the basolateral membrane infoldings and apical tight junctions (Kierszenbaum and Tres, 2015). The stroma is the connective tissue between the basolateral membrane and the capillary endothelium, which surrounds CPx with its components, for example, collagen fibrils, various cells including fibroblasts, pial cells, stromal macrophages, and dendritic cells (Kaur et al., 2016).

Stromal macrophages are suggested to enter the intraventricular area via the following pathways: the paracellular transport that passes through the intercellular spaces inside the epithelial sheet; the transcellular transport that passes through CPx epithelial cells. CPx-related intraventricular macrophages can be detailed as follows: free-floating cells are buoyant in the fluid, whereas supraependymal cells are reported to rest in close proximity to the ependymal cells; and epiplexus cells, also known as Kolmer's cells named by the researcher first described, are associated with the microvilli of the epithelial layer.

The amount of the CSF secreted by CPx is approximately 400-600 ml/day or 0.3-0.6 ml/min/g with an estimated volume of approximately 150 ml in adults (Sakka, Coll and Chazal, 2011; Prabhakar, 2017). Its volume may differ with age due to the renewal time. Although the main pathway of CSF production is obtained with choroidal secretion; the brain extracellular fluids, cerebral blood vessels around the blood-brain barrier (BBB), and also ependymal cells contribute to CSF as extrachoroidal secretion which appears to be less significant.

CSF production and reabsorption cycles are as follows: the produced CSF from the lateral ventricles passes through the interventricular foramen and flows into the third ventricle and then into the fourth ventricle through the cerebral aqueduct (of Sylvius); concurrently, most of CSF passes from the median aperture to the lateral aperture through the cisterns of the subarachnoid space, and the circulation ends at the superior sagittal sinus; furthermore, CSF is transferred to the venous blood system via the arachnoid villi, composed of a thin layer of endothelium, which are projected from the arachnoid mater (Dziegielewska et al., 2001).

There are two stages of CSF production: passive filtration into the choroidal interstitium, and active secretion into the ventricles including the transport of Na+, K+, HCO3- ions, and water (Orešković, Radoš and Klarica, 2017). Except for the choroidal epithelial cells regulating the chemical composition of CSF, there are another two ependymal cell types, tanycytes and ependymocytes,

which affect CSF dynamics. While the ependymocytes allow molecule transition between CSF and the neurons, the tanycytes of circumventricular organs take part in responding to changes in blood-derived hormone levels (Wolburg and Paulus, 2010; Rea, 2015).

2.2. Functions and Dysfunctions of the Choroid Plexus

CSF is produced by ependymal cells and originates from the arterial blood of CPx. This fluid fills the brain ventricles, the subarachnoid space, and the central canal in the medulla spinalis. The ependymal tissue separates CPx from the cerebral ventricles and filters water and other substances, which become contents of CSF (Bailey, 2019).

CPx has two important functions: (a) supporting brain development and (b) preserving the developing structure. It performs these functions by protecting the brain through the blood-CSF barrier and producing the CSF. Sufficient CSF production by CPx supports and secures the brain and the spinal cord and has an important role in removing waste. With the support of the arachnoid layer, the CSF prevents the leakage of blood and other molecules in case of perforation in the brain vessels. The blood-CSF barrier and BBB are important in preventing the transport of toxic substances to CNS. CPx contains cells involved in body defense, such as macrophages, dendritic cells, and lymphocytes. Microglia and other immune system cells can enter the CNS through CPx. The intense presence of these cells in CPx and the blood-CSF barrier are critical in preventing pathogens from entering the brain (Bailey, 2019).

CNS pathologies such as multiple sclerosis and neurodegenerative diseases, infections, brain injury, and trauma, result in oxidative stress, which in turn leads to various inflammatory processes. Moreover, these pathologies are responsible for the production of many chemokines and cytokines and the breakdown of the BBB and the blood-CSF barrier. Stromal macrophages and dendritic cells are thought to present antigens to T lymphocytes, which enter the CSF from the broken-down BBB and the blood-CSF barrier (Stridh, Ek, Wang, Nilsson, and Mallard, 2013; Coisne and Engelhardt, 2011).

CPx pathology is usually linked with the flow and production of CSF volume. The flow pathways of CSF flow-pathway can become narrowed due to different pathologies; and as a result, the flow slows down, distension increases, and hydrocephalus occurs. Tumors associated with ventricles and CPx are as follows; ependymomas, mostly seen in pediatric cases; malign carcinoma; benign (mostly) papilloma of CPx; colloid cysts. On the other hand, the other obstruction problems include cysts of posterior fossa, Dandy-Walker syndrome, the fourth ventricle malformation consisting of atresia of foramen Magendie as well as atresia of foramen Luschka, hypoplasia of the cerebellar structures. Subarachnoid cistern obliteration or arachnoid villi dysfunction can cause hydrocephalus, although hydrocephalus may be also associated with spina bifida cystica that may not be detected at birth. Hydrocephalus results in thinning of calvaria bones, prominence of the forehead, cerebral cortex and white matter atrophy, and basal ganglia and diencephalon compression (Moore et al., 2016). Cell-based therapies are being studied to present

ideal therapeutic strategies for treating many CNS diseases (Lehtinen, Bjornsson, Dymecki, Gilbertson, Holtzman and Monuki, 2013).

3. CONCLUSION

CPx, which is responsible for the synthesis and regulation of CSF secretion, plays a crucial role in CNS maturation and maintaining the balanced continuum of hemodynamics. Diagnosis and treatment approaches for CNS pathologies, such as congenital malformations, tumorigenesis, inflammation, and degeneration, will be further enhanced when the anatomical, embryological, and histological features of CPx are detailed and understood.

REFERENCES

Moore, K. L., Persaudi T. V. N., Torchia, M. G. (2016). The Developing Human-E-Book:Clinically Oriented Embryology. 11th ed. Elsevier Health Sciences

Friedrich, P., Jens, W. (2018). Sobotta Atlas of Anatomy Vol. 3 Head, Neck and Neuroanatomy. 16th ed. Elsevier GmbH

Felten, D. L., O´banion, M. K., Maida, M. S. (2015). Netter's Atlas of Neuroscience. 3rd ed. Elsevier Health Sciences, 105–131.

Sadler, T. W. (2014) Langman's Medical Embryology. 13th ed. USA: Lippincott Williams&Wilkins/Wolters Kluwer Health

Gupta, D. (2017). Neuroanatomy. In: Essentials of Neuroanesthesia. Elsevier, 3–40.

Catala, M. (2019). Development of the Cerebrospinal Fluid Pathways During Embryonic and Fetal Life in Humans. In: Pediatric Hydrocephalus. Cham: Springer International Publishing, 139–195.

Ghersi-Egea, J-F., Strazielle, N., Catala, M., Silva-Vargas, V., Doetsch, F., Engelhardt, B. (2018). Molecular anatomy and functions of the choroidal blood-cerebrospinal fluid barrier in health and disease. Acta Neuropathologica, 135(3), 337–361.

Kierszenbaum, A. L., Tres L. L. (2015). Histology and Cell Biology An Introduction to Pathology. 4th ed. Saunders

Pawlina, W., Ross, M. H. (2018). Histology: a text and atlas: with correlated cell and molecular biology. Lippincott Williams & Wilkins.

Mescher, A.L. (2016). Junqueira's Basic Histology Text & Atlas. 14th ed. McGraw-Hill Education, 295–304.

Netsky, M.G., Shuangshoti S. (1975). The Choroid Plexus in Health and Disease. Butterworth-Heinemann. Elsevier.

Dziegielewska, K. M., Ek, J., Habgood, M. D., Saunders, N. R. (2001). Development of the choroid plexus. Microscopy Research and Technique. 52(1), 5–20.

Kaur, C., Rathnasamy, G., Ling, E-A. (2016). The Choroid Plexus in Healthy and Diseased Brain. Journal of Neuropathology & Experimental Neurology, 75(3), 198–213.

Liddelow, S. A. (2015). Development of the choroid plexus and blood-CSF barrier. Frontiers in Neuroscience, 9.

Lun, M. P., Monuki, E. S., Lehtinen, M. K. (2015). Development and functions of the choroid plexus–cerebrospinal fluid system. Nature Reviews Neuroscience, 16(8), 445–457.

Kovacs, G. G. (2018). Cellular reactions of the central nervous system. In: Handbook of Clinical Neurology. Elsevier B.V, 13–23.

Sakka, L., Coll, G., Chazal, J. (2011). Anatomy and physiology of cerebrospinal fluid. European Annals of Otorhinolaryngology, Head and Neck Diseases. 128(6), 309–316.

Prabhakar, H. (2017). Essentials of neuroanesthesia. Essentials of Neuroanesthesia.

Orešković, D., Radoš, M., Klarica, M. (2017). Role of choroid plexus in cerebrospinal fluid hydrodynamics. Neuroscience. 354, 69–87.

Wolburg, H., Paulus, W. (2010). Choroid plexus: biology and pathology. Acta Neuropathologica, 119(1), 75–88.

Rea, P. (2015). Essential Clinical Anatomy of the Nervous System. 1st ed. Essential Clinical Anatomy of the Nervous System. Academic Press

Bailey, R. (2019). Choroid Plexus Location, Structure, and Function. ThoughtCo

Stridh, L., Ek, C. J., Wang, X., Nilsson, H., Mallard, C. (2013). Regulation of Toll-Like Receptors in the Choroid Plexus in the Immature Brain After Systemic Inflammatory Stimuli. Translational Stroke Research, 4(2), 220–227.

Coisne, C., Engelhardt, B. (2011). Tight Junctions in Brain Barriers During Central Nervous System Inflammation. Antioxidants & Redox Signaling, 15(5), 1285–1303.

Lehtinen, M. K., Bjornsson, C. S., Dymecki, S. M., Gilbertson, R. J., Holtzman, D. M., Monuki, E. S. (2013). The Choroid Plexus and Cerebrospinal Fluid: Emerging Roles in Development, Disease, and Therapy. Journal of Neuroscience, 33(45) , 17553–17559.

Table 1: Histological Alterations During Choroid Plexus Development From Different Sources (12–15)				
Type	**Young Form**	**Intermediate Form**		**Adult Form**
Stage	I	II	III	IV
Week	7th	9th	17th	29th
Epithelial layer	High Pseudostratified epithelium	High to low columnar (to cuboidal) epithelium	Cuboidal epithelium (flattened cells)	Cuboidal to squamous epithelium
Nuclei of epithelial cells	Central located	Apical located	Central or apical located (stage III cells with high glycogen) Basal located (progressing to stage IV cells with low glycogen)	Basal located (mostly stage IV cells) or central located (remaining stage III cells)
Brush Border Microvilli	Present	Present	Present	Present

Villous Elaboration	Not present	Villus-like projections	Distinct apical villi	Complex multiple villi with fronds
Glycogen Content	Lacks	Abundant	Moderate to Diminished	Minimal or Lacks

Legends for Figures

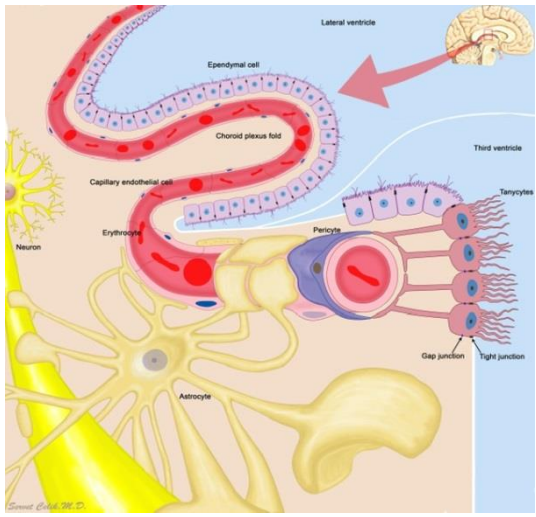

Figure 1 Illustration shows the relationship between ependymal cells and cellular images of 3rd and 4th ventricles and other structures

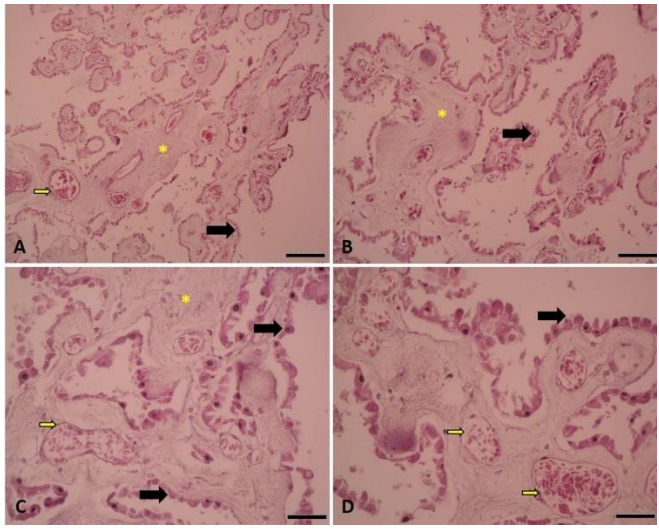

Figure 2 A-D Choroid plexus sections obtained from human cadaver. X10-X20-X40 magnification. H&E staining. Yellow arrow capillary vessel; yellow asterix tela choroidea, interstitial connective tissue, and black arrow ependymal cells.

Ependymal cells are seen separately from the basal lamina in a long-time fixated specimen

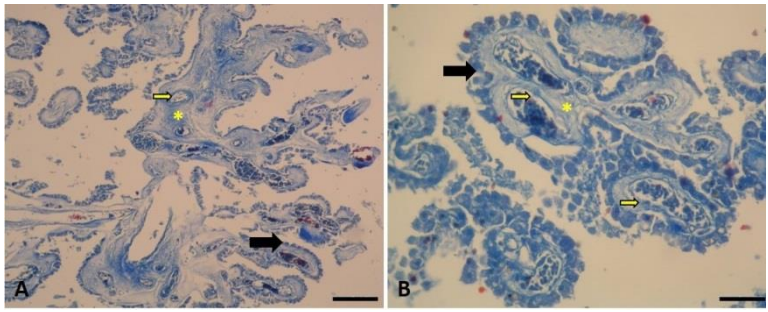

Figure 3 A, B Choroid plexus sections obtained from human cadaver. X10-X40 magnification. Mallory azan staining. Yellow arrow capillary vessel; yellow asterix tela choroidea, interstitial-connective tissue; and black arrow ependymal cells

CHAPTER 4

PEDIATRIC FEMORAL SHAFT FRACTURES CURRENT APPROACHES

Fevzi BIRIŞIK[1] MD
Yücel BILGIN[2],MD

[1] Health Sciences University, Istanbul Education and Research Hospital, Orthopedics and Traumatology Department, Istanbul, Turkey, dr.fevzibirisik@gmail.com . ORCID ID: 0000-0003-3274-6096
[2] Health Sciences University, Istanbul Education and Research Hospital, Orthopedics and Traumatology Department, Istanbul, Turkey, yucelbilgin70@hotmail.com. ORCID ID: 0000-0003-0433-1918

INTRODUCTION

In the pediatric population, there is another increase in the frequency of cuts in this age group in parallel with the encouragement of participation in more activities and sports activities. Similarly, the incidence of fractures increases in pediatric femoral fractures, especially in shaft fractures.

It has been reported that the frequency of pediatric femoral shaft fractures is between 16 and 19 per 100,000 population annually and its rate among all pediatric fractures is around 2% (Heideken et al. 2011; Hinton et al. 1999). The age group in which it is observed more frequently is observed as two peaks, 2-3 years and adolescent period (Hedlund et al. 1986; Kuremsky et al. 2007).

It is more common in boys than in girls, and the incidence of shaft fractures is more common than distal and proximal femur fractures (Loder et al. 2006).

It has been reported that femoral fractures show a bimodal seasonal frequency throughout the year in the pediatric age group, and their frequency increases especially in the summer and late winter periods (Heideken et al. 2011).

For the patient and his family, it requires hospitalization and treatment in terms of shortening the duration of disability and less psychological and physical stress (Henderson et al. 1992). Nowadays, with the advancing modern treatments, it is seen that the desire for earlier

mobilization and ease of care have increasingly brought surgical treatment to the fore.

1.ETIOLOGY AND INJURY MECHANISM

Observation of femoral shaft fractures in children who have not yet gained the ability to walk, especially children under the age of 1, requires evaluation in terms of child abuse (Gross et al. 1983).

It should be kept in mind that the trauma story conveyed by the family arouses suspicion, unclear statements, and unusual situations such as late admission to the hospital that warns the clinician for child abuse.

It has been reported that ecchymotic lesions at different healing stages in the extremities and different parts of the body, skin burns, and the presence of multiple fractures in the patient may be symptoms of child abuse (Kocher et al. 2010). In addition, another cause of femoral shaft fractures in children under 1 year of age may be metabololic bone diseases (Miller et al. 2019; Wood et al. 2014).

Pathologically, fractures may develop after osteogenesis imperfecta, cerebral palsy and osteoporosis secondary to meningomyelocele, which cause widespread osteopenia in children.

High-energy traumas such as frequent falls in younger age groups and traffic accidents in adolescence cause femoral shaft fractures (Heideken et al. 2011).

Other causes of pediatric femoral shaft fractures were stated to be due to pathological fractures caused by tumoral lesions, exposure to

radiation and its occurrence after implant removal (Kong et al. 2014), and stress fractures after overuse (Price et al. 2010).

2.CLINICAL EVALUATION

A careful evaluation is important during admission to the hospital, especially in younger children who cannot express themselves. Being alert for accompanying cranial and internal organ injuries is essential in terms of life-threatening and medicolegal. Similarly, minor traumas that may occur in extremities other than the focal extremity may be overlooked.

Taking a detailed history from the patient and his family will provide clinical convenience in the diagnostic approach. Having a suspicious history, inconsistency between the history and physical examination, and frequent traumas should be considered in terms of abuse. Examination of the entire limb as a whole; should include skin lesions, range of motion, and neurovascular examination. There may be pathological movement in the injured extremity after fracture. The traumatic limb should be compared with the contralateral limb.

Deformity, swelling and tenderness, discoloration and inability to walk are the main findings observed in the thigh and leg during physical examination. Shortness of the extremity can be seen.

The hip and knee joints of the affected femur should be included in the examination as they may involve accompanying injuries.

Vital signs of the patient should always be evaluated. Findings such as detected hypotension and anemia definitely require further

investigation. The reason for this can be explained by an accompanying injury (Levy et al. 2005; Unal et al. 2006).

3.RADIOLOGICAL EVALUATION

3.1.Direct x-ray (X-ray); The first step in the radiological evaluation of pediatric femoral shaft fractures is direct roentgenography. Antero-posterior and lateral radiographs taken for this purpose will often provide sufficient information. Despite the possibility of accompanying lying, it would be appropriate to have radiography taken to visualize the hip joint and knee joint. X-ray should be seen before and after initial stabilization.

3.2.Computed tomography (CT): Although it is not necessary in isolated femoral shaft fractures, it may contribute to the evaluation of accompanying joint fractures and physical injuries.

3.3.Magnetic resonance imaging (MRI): In isolated femoral shaft fractures, it can provide additional information in the etiology of stress fracture or in the presence of a tumoral lesion causing pathological fracture. It is useful in adjacent joint injuries, showing intra-articular pathologies, ligament injuries.

3.4.Scintigraphy: Provides additional information in stress fractures and pathological fractures. Its use is not common**.**

4. CLASSIFICATION

Pediatric femoral diaphyseal fractures are classified according to the AO pediatric long bone fractures classification. According to this classification, femoral diaphyseal fracture is coded with 32. The

fracture is coded as simple and transverse with 32-D / 4.1, and the fracture with multifragmentary and transverse with 32-D / 4.1. The fracture is coded with 32-D / 5.1 if it is simple and oblique or spiral, and 32-D / 5.2 if the fracture is multifragmentary oblique or spiral (AO Pediatric Comprehensive Classification of Long Bone Fractures (PCCF). 2018).

Pediatric femoral diaphyseal fractures were classified according to treatment by the American Academy of Orthopedic Surgeons (AAOS) in 2020. According to this classification, they defined 5 different classes. Class 1 was defined as “Protect Until Healed”. Class 2 was defined as “Actice Cast Treatment”. Class 3 was defined as “Flexible Fixation”. Class 4 was defined as “Rigid Fixation”. Class 5 was defined as “Limb/Life Preservation” (Weltsch et al. 2020). The relationship between the current classification and treatment will be explained in the treatment section.

Open fractures are classified with the Gustilo classification (Gustilo R. 1987).

5. TREATMENT

Treatment in pediatric femur fractures is determined by age and fracture type. Conservative treatment methods such as Pavlik bandage and spica casting and surgical treatment methods such as elastic nailing, submuscular plate screw application and external fixation can be applied.

5.1. Conservative Treatment

Conservative treatment is recommended for Class 1 and Class 2 fractures according to the AAOS classification of pediatric femoral fractures. Class 1 includes all femoral diaphyseal fractures of patients younger than 6 months, and incomplete or complete nondisplaced fractures of patients aged 6 months to 4 years. Class 2 includes displaced or shortened fractures of patients aged 6 months to 4 years. Pavlik bandages are used in patients younger than 6 months in Class 1 fractures. In the conservative treatment of Class 1 and Class 2 patients aged 6 months to 4 years, preferably walking/regular spica cast method is used (Weltsch et al. 2020).

In the routine spica casting technique, the patient is seated on a casting table under anesthesia. The extremity is wrapped and supported with pads. By applying traction, cast is made with the ankle, knee, hip at 90 degrees of flexion, the hip at 30 degrees of abduction and the thigh at 15 degrees of external rotation. In the spica walking cast technique, cast is made when the knee is in 50 degrees of flexion, the hip is in 45 degrees of flexion and 15 degrees of external rotation (Flynn ve Skaggs, 2010). Spica cast can be made from both traditional and synthetic fiberglass materials. Cast fractures are a common problem (Özdemir ve Deveci, 2018). Although it varies according to age, angulation up to 20 degrees in the coronal plane and 30 degrees in the sagittal plane after the cast is acceptable (Buehler et al. 1995). (Figure-1a, b)

Figure 1 a-Radiography with a diagnosis of Class 1 pediatric right femur fracture. b-Radiography after spica cast application

5.2. Surgical Treatment

Surgical treatment is recommended for Class 3, Class 4 and Class 5 fractures according to the AAOS classification of pediatric femoral fractures. Class 3 includes patients above 4 years of age with a simple femoral diaphyseal fracture with no skeletal maturity. Flexible intramedullary nailing technique is used in the treatment of these patients. Class 4 includes pediatric patients over 4 years of age with complex femoral diaphyseal fractures. In these fractures, submuscular plating or external fixation technique can be used in patients aged 4-9 years, rigid nailing with trochanter entry, submuscular plating or external fixation technique can be used in patients over 9 years old. Class 5 includes pediatric patients with femoral diaphyseal fractures

accompanied by systemic hemodynamic instability, multitrauma, mangled extremity, contaminated high-energy open fracture or vascular injury. In these patients, early full care with rigid fixation, or damage control orthopedic surgery with temporary external fixator application can be applied (Weltsch et al. 2020).

The most commonly used surgical method in the treatment of pediatric femoral diaphyseal fractures is flexible intramedullary nailing (Figure-2a, b, c, d). Titanium elastic nails are used in the flexible intramedullary nailing technique. It is usually applied by retrograde method. One window is opened to the medial and lateral of the femur, in the proximal part of the distal femur physis. After proper fracture reduction is achieved with traction, elastic nails are placed through these windows. The thickness of the elastic nail to be used is determined by multiplying the thickness of the intramedullary canal in the femoral diaphysis by 0.4 (Flynn ve Skaggs, 2010). In a 2018 article, 48 patients treated with flexible intramedullary nailing with the diagnosis of femoral diaphyseal fracture were retrospectively reviewed. Union was observed in all fractures in 9-12 weeks. Excellent results were reported in 83 percent of patients. Soft tissue irritation around the knee due to nails was the most common complication. In addition, shortness, varus malunion, surgical site infection and nail migration were detected as other complications (Govindasamy et al. 2018).

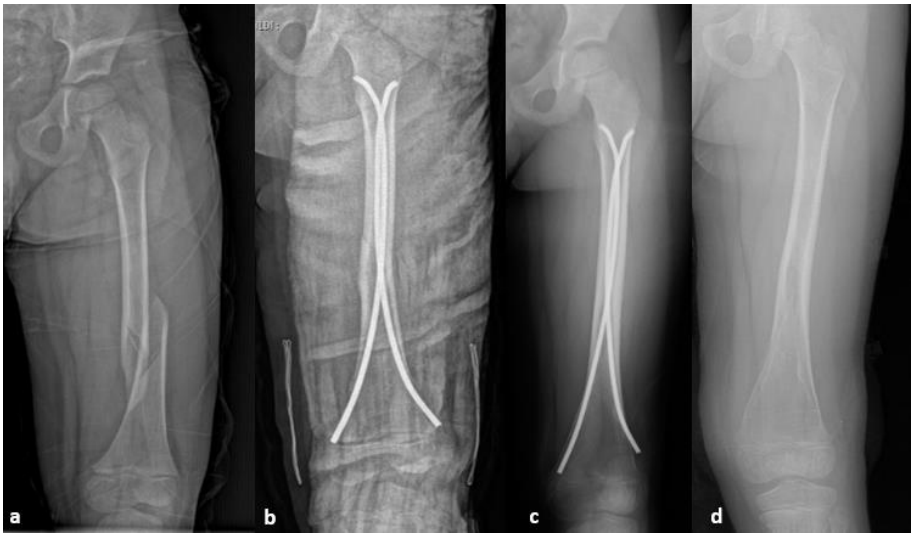

Figure 2 a-Radiography with a diagnosis of Class 3 pediatric left femur fracture.
b-Radiography after flexible intramedullary nailing surgery.
c- Radiography after union.
d- Radiography after removal of flexible intramedullary nails.

External fixators and submuscular plating are other methods that can be used in the treatment of pediatric femoral diaphyseal fractures (Figure-2a,b,c,d). They are preferred in the treatment of Class 4-5 complex femoral diaphyseal fractures. External fixators are more prominent in fractures with more soft tissue injury. However, pin bottom infections are the most important complications. In an article published in 2014, 31 pediatric femoral fracture patients treated with an external fixator were retrospectively reviewed. The average follow-up period with fixators was found to be 17 weeks. Refracture developed in only one patient during follow-up. As a complication, leg length discrepancy of more than 2 cm in one patient and peronel nerve palsy in 1 patient were detected (Kong ve Sabharwal, 2014). In

the light of the current literature, external fixators are a recommended method in the treatment of unstable complex pediatric femoral fractures accompanied by soft tissue injury. Submuscular plating can be used in the treatment of unstable pediatric femoral diaphyseal fractures. Especially in school-age children and patients with narrow medullary canal, it is an advantage (Li ve Hedequist, 2012).

Figure 3 a-Radiography with a diagnosis of Class 4 pediatric left femur fracture.
b-Radiography after external fixation surgery.
c- Radiography after union.
d- Radiography after removal of external fixator.

6. COMPLICATIONS

The most important complications identified after pediatric femur fractures are; leg length inequality, compartment syndrome, neurovascular injury, delayed union, malunion and infection (Flynn ve Skaggs, 2010).

CONCLUSION

Femoral diaphyseal fractures are an important health problem in the pediatric population. Mobility decreases and education can affect children. The possibility of child abuse should always be kept in mind in the etiology. Physical examination and radiological examinations are usually sufficient for diagnosis. While classifying fractures, AAOS classification comes to the fore in the current literature. Conservative methods are in the foreground in the treatment of femoral diaphyseal fractures aged 4 and under. Conservative methods are in the foreground in treatment. The most commonly used conservative method is spica cast. Surgical methods come to the fore in the treatment of pediatric femoral fractures over the age of 4. The most common surgical method is flexible intramedullary nailing. External fixators, submuscular plating and rigid nails with trochanter entry can be used in unstable fractures. The most important complications identified after pediatric femur fractures are; leg length inequality, compartment syndrome, neurovascular injury, delayed union, malunion and infection.

REFERENCES

AO Pediatric Comprehensive Classification of Long Bone Fractures (PCCF). (2018). Journal of orthopaedic trauma, 32 Suppl 1, S117–S140.

Buehler KC, Thompson JD, Sponseller PD, Black BE, Buckley SL, Griffin PP.(1995). A prospective study of early spica casting outcomes in the treatment of femoral shaft fractures in children. J. Pediatr Orthop, 15(1), 30-5.

Flynn JM, Skaggs DL. (2010). Femur Diaphysis Fractures. Rockwood and Wilkins Fractures in Children, 7th Edition, Eds: Beaty JH, Kasser JR, Philadelphia, 17, 656-67.

Govindasamy, R., Gnanasundaram, R., Kasirajan, S., Ibrahim, S., & Melepuram, J. J. (2018). Elastic Stable Intramedullary Nailing of Femoral Shaft Fracture-Experience in 48 Children. The archives of bone and joint surgery, 6(1), 39–46.

Gross RH, Stranger M.(1983). Causative factors responsible for femoral fractures in infants and young children. J Pediatr Orthop.3:341-343.

Gustilo R. B. (1987). Current concepts in the management of open fractures. Instructional course lectures, 36, 359–366.

Hedlund R, Lindgren U.(1986) The incidence of femoral shaft fractures in children and adolescents. J Pediatr Orthop. 6(1):47–50.

Heideken J, Svensson T, Blomqvist P, Haglund-Akerlind Y, Janarv PM. (2011). Incidence and trends in femur shaft fractures in Swedish children between 1987 and 2005. J Pediatr Orthop. 31:512–519.

Henderson J, Goldacre MJ, Fairweather JM and Marcovitch H. (1992). Conditions accounting for substantial time spent in hospital in children aged 1-14 years. Arch Dis Child. 67: 83-86.

Hinton RY, Lincoln A, Crockett MM, Sponseller P, Smith G.(1999). Fractures of the femoral shaft in children. Incidence, mechanisms, and sociodemographic risk factors. J Bone Joint Surg Am. 81:500–509.

Kocher MS, Sink EL, Blasier RD, Luhmann SJ, Mehlman CT, Scher DM, Matheney T, Sanders JO, Watters WC 3rd, Goldberg MJ, Keith MW, Haralson RH 3rd, Turkelson CM, Wies JL, Sluka P, McGowan R.(2010). American Academy of Orthopaedic Surgeons.. American Academy of Orthopaedic Surgeons clinical practice guideline on treatment of pediatric diaphyseal femur fracture. J Bone Joint Surg Am. 92(8):1790–2.

Kong, H., Sabharwal, S. (2014). External fixation for closed pediatric femoral shaft fractures: where are we now?. Clinical orthopaedics and related research, 472(12), 3814–3822.

Kuremsky MA, Frick SL. (2007). Advances in the surgical management of pediatric femoral shaft fractures. Curr Opin Pediatr. 19:51–57.

Levy BA, Zlowodzki MP, Graves M, Cole PA. (2005). Screening for extermity arterial injury with the arterial pressure index. Am J Emerg Med. 23(5):689–95.

Li, Y, Hedequist, D. J. (2012). Submuscular plating of pediatric femur fracture. The Journal of the American Academy of Orthopaedic Surgeons, 20(9), 596–603.

Loder RT, O"Donnell PW, Feinberg JR. (2006). Epidemiology and Mechanisms of Femur Fractures in Children. J Pediatr Orthop. 26:561–6.

Miller M, Stolfi A, Ayoub D. (2019). Findings of metabolic bone disease in infants with unexplained fractures in contested child abuse investigations: a case series of 75 infants. J Pediatr Endocrinol Metab. 32:1103–20.

Özdemir G, Deveci A. (2018). Pelvipedal Alçılama. Totbid Derdisi, 17, 296-299.

Price CT, Herrera-Soto J. (2010). Extra-articular injuries of the knee. In: Beaty JH, Kasser JR. Rockwood and Wilkins' Fractures in Children. Philadelphia PA: Walter Klower/Lippincott, William and Wilkins; pp.842–885.

Unal VS. Gulcek M, Unveren Z, Karakuyu A, Ucaner A.(2006). Blood loss evaluation in children under the age of 11 with femoral shaft fractures patients with isolated versus multiple injuries. J Trauma. 60(1):224–226

Weltsch, D., Baldwin, K. D., Talwar, D., & Flynn, J. M. (2020). Expert Consensus for a Principle-based Classification for Treatment of Diaphyseal Pediatric Femur Fractures. Journal of pediatric orthopedics, 40(8), e669–e675.

Wood JN, Fakeye O, Mondestin V, Rubin DM, Localio R, Feudtner C. (2014). Prevalence of abuse among young children with femur fractures: a systematic review. BMC Pediatr. 14:169.

CHAPTER 5

INVESTIGATION OF THE OXIDATIVE STRESS AND APOPTOSIS IN SEVERE PREECLAMPSIA

Res. Asist. MD. Emel OZTURK[1],
Assist. Prof. Dr. Reyhan GUNDUZ[2]

[1] Harran University, Faculty of Medicine, Histology-Embriology Department, Sanlıurfa, Turkey. malatya44emel@hotmail.com, Orcid ID: 0000-0003-0756-0329
[2]Dicle University, Faculty of Medicine, Gynecology and Obstetrics Department, Diyarbakır, Turkey. ryhn.gunduz@gmail.com, Orcid ID: 0000-0001-8468-7038

OBJECTIVES: Preeclampsia is a common pregnancy specific disease with potential adverse maternal and neonatal outcome, that affects 3–5% of all pregnancies. The etiology of preeclampsia has not been fully clarified. Several molecular markers of preeclampsia were investigated in the past; but, the importances of apoptosis and oxidative stress were not well documented. We aimed to determine the apoptosis, antioxidant status and oxidative stress in healthy and severe preeclamptic umbilical tissues.

METHODS: 30 patients were included in the study, 15 pregnants were control and 15 pregnants were severe preeclampsia at Gaziantep University Şahinbey Research and Application Hospital Department of Obstetrics and Gynecology. MDA, CAT, GPx, TAS, TOS were evaluated by elisa. The umbilical tissues of pregnant women were taken during delivery for western blot and immunohistochemical analysis. Caspase 3 antibody was examined using western blot and immunohistochemia.

RESULTS: The elisa analyses showed that levels of MDA and TOS were higher in severe preeclampsia compared to healthy pregnant women. However, levels of CAT, GPx and TAS were lower in severe preeclampsia group compared to control group. The immünohistochemia and western blot analyses showed that the expression of the protein Caspase 3 was significantly higher in the umbilical tissues of women with severe preeclampsia than in the umbilical tissues of control women.

CONCLUSIONS: Upregulation of MDA, TOS and downregulation of CAT, GPx and TAS were consistent with apoptosis in the severe preeclampsia umbilical cords. These results may contribute to the pathophysiology of severe preeclampsia.

1. INTRODUCTION

Preeclampsia (PE), more than simply gestational hypertension during pregnancy, is a leading cause of preterm delivery and of maternal mortality and morbidity worldwide, (Duley L, 2009; Lisonkova S, 2014). It is characterized by long duration proteinuria, hypertension and other adverse conditions in the second half of pregnancy (Ahmad IM, 2019; Gupta S, 2009).

Oxidative stress, often referred to as an imbalance between reactive oxygen species (ROS) and antioxidants, increases during severe preeclampsia (S.P) and results in increased production of lipid peroxides and ROS, such as superoxide ($O2^{-}$) (Hsieh TT,2012; Elliot MG, 2016). Oxidative stress is a known cause of endothelial dysfunction making it a potential contributor to preeclampsia (Gupta S, 2005; Abad C, 2012).

Apoptosis has a major function in most defending mechanism such as immune reaction triggered when cells are injured by a disease or dangerous agents. Researchers have reported that there are two essential apoptotic pathways: the intrinsic which is widely known mitochondrial pathway and the extrinsic or death receptor pathway. The intrinsic and extrinsic reach to same destination—execution

pathway (Öztürk E, 2020). This pathway starts with the activation of Caspase 3, which is an initiator of apoptosis and characterized by DNA fragmentation, apoptotic body formation, degeneration of cytoskeletal and nuclear proteins, and production of antigens for receptors of phagocytic cells (Martinvalet D, 2005). Proliferation and apoptosis are requisite components of the trophoblast life cycle. There are abnormal cell turnover including an increased apoptosis in placental villous trophoblast of severe preeclamptic pregnancies (Ishihara, N, 2002).

Several molecular markers of preeclampsia were investigated in the past; but, the importances of apoptosis and oxidative stress were not well documented. This study was aimed to investigate the apoptotic marker Caspase 3, total antioxidant status and oxidative stress in the umbilical tissues of patients with severe preeclampsia.

2. MATERIAL AND METHODS

The study protocol was accepted by the Gaziantep University's Human Ethics' Committee with number 2014/305. This study was carried out on umbilical tissues taken from 30 women aged between 25-30 who applied to Gaziantep University Şahinbey Research and Practice Hospital, Department of Obstetrics and Gynecology after delivery. The study was conducted in Gaziantep University Faculty of Medicine, Histology-Embryology Department Laboratory.

2.1. Elisa Assay

For this, umbilical tissue samples stored at -80 were used. The samples were homogenized on ice, then centrifuged to remove supernatants. These supernatants were used for ELISA analysis. Analyzes were made according to the manufacturer's instructions CAT (201-12-5456, Sunred Biological Technology Co., Ltd., 96 Wells Elisa kit, Shanghai, Chına), MDA (No. MBS772388, , MyBioSource), GPx (No MBS167041, MyBioSource), TAS (No. 201-12-7412, Sunred Biological Technology Co., Ltd., 96 Wells Elisa kit, Shanghai, Chına) and TOS (No. 201-12-5807, Sunred Biological Technology Co., Ltd., 96 Wells Elisa kit, Shanghai, Chına).

2.2. Tissue Tracking

Umbilical tissue fragments taken after birth were fixed in 10% neutral formalin solution for 10 days. It was divided into pieces of suitable size for tissue follow up and taken into lidded cassettes. The tissues were washed in running water for 1 hour to clear the fixative solution. Water removed by passing through increasingly graded alcohols. Paraffin blocks were prepared by paraffin inclusion after transparentization with xylene. 5 micrometer thick sections were cut from the blocks using a Leica RM 2145 model microtome and prepared for staining.

2.3. Immunohistochemical Analysis

The sectioned praparates were passed through xylene series after waiting at least two hours in a 65-70 degree oven. Then it was passed through the decreasing alcohol series, placed in distilled water and placed in a citrate buffer, and then put in the microwave for 10 minutes for antigen recovery and cooled at room temperature for 10 minutes. Ultraviole V block was instilled after H_2O_2 was taken. Caspase 3 primary antibody was dropped and kept at +4 overnight. The next morning, it was taken into the secondary antibody, streptavidin HRP was dropped, and after the DAB solution, it was passed through the alcohol and xylene series again, and finally it was covered with a coverslip using entellan. Image J program was used for immunoreactivity.

2.4. Western Blot Analysis

Umbilical tissues were homogenized and lysed in radioimmunoprecipitation assay buffer supplemented with 1 mM phenylmethanesulfonyl fluoride for 1 h and then centrifuged at 15 000 r.p.m. for 30 min at 4 °C. The protein concentration was measured using a BCA protein assay kit. Equal amounts of protein (40 μg per lane) were separated on 10% SDS–polyacrylamide gels and then transferred onto polyvinylidene fluoride membranes (Millipore, Bedford, MA, USA). The membrane was blocked in Tris-buffered saline containing 5% nonfat milk powder for 1 h and then incubated overnight with Caspase 3 antibodie, each diluted in Tris-buffered saline 5% nonfat milk powder; the sample was subsequently incubated

with an antibody against beta actin (β-actin) as a loading control. The membrane was washed three times with Tris-buffered saline containing Tween-20 and then incubated with horseradish peroxidase-conjugated anti-rabbit IgG (1:1500) for 1 h at room temperature. Protein was detected by enhanced chemiluminescence reagents. The level of expression of the protein was analyzed using ImageJ software.

3. STATISTICAL ANALYSIS

All statistical analyses were carried out by using GraphPad Prism version 7.00 for Mac, GraphPad Software, La Jolla, California, USA. D'Agostino Pearson omnibus test was used to identify the normal distribution of the data. In the case of normal distribution, quantitative variables were compared using one-way analysis of variance (ANOVA) and Tukey's posthoc test. Kruskal Wallis test and Tukey's post-hoc test were used for comparing the quantitative with the abnormal distribution. The data were expressed as the mean of normalized data±standard deviation of the mean. $p<0.05$ was considered as statistically significant.

4. RESULTS

4.1. Characteristics Of The Working Groups

In our study, no statistically significant difference was observed between the ages of normal and severe preeclampsia pregnant women ($p>0.05$). However, when we looked at gestational age at birth (weeks), fetal birth weight, systolic blood pressure (mm Hg) and diastolic blood pressure (mm Hg), it was observed that there was a

statistically significant difference between the two groups (p<0.05). Also, Also, when we looked at uric acid and urine protein in the urine of these two groups, it was observed that there was a significant increase in the S.P group (p<0.05) (Table 1).

Table 1. Characteristics Of Working Groups

	Control	S.P	*p*
Age	29.3 ± 1.2	29.5 ± 2.7	0.692
Gestational age at birth (weeks)	39.2 ± 1.1	28.3 ± 2.3	0.015
Systolic blood pressure (mm Hg)	115.5 ± 6.7	161.9 ± 7.8	0.001
Diastolic blood pressure (mm Hg)	72.3 ± 4.8	112.5 ± 6.9	0.001
Uric acid	323.5± 92.1	458.7± 110.4	0.001
Urine protein/24 h	-	4.9 ± 3.4	0.001
Fetal birth weight	3199.2± 300.2	1836.3± 856.4	0.001

When we look at the age ratio of the groups included in the study; There was no significant difference between severe preeclampsia pregnant women and healthy control group. However, systolic, diastolic blood pressures, uric acid and urine protein were significantly higher in severe preeclampsia groups than in the control group. In addition, Fetal birth weight was lower in severe preeclampsia groups than in the control group. (p <0.001) (Table 1).

4.2. Biochemical Findings

Table. 3: MDA, CAT, GPx, TAS and TOS levels in groups.

Groups	Control	S.P	*p*
MDA levels (nmol/l)	0.23 ± 0.18	0.80± 0,11	0.0001
CAT levels (nmol/l)	1.78 ± 1.04	1.28 ± 0.42	0.0016
GPx levels (nmol/l)	2.14 ± 1.21	1.39± 1.05	0.0028
TAS levels (nmol/l)	2.95 ± 0.11	2.11 ± 0.57	0.0094
TOS levels (nmol/l)	3.78 ± 1.23	7.97 ± 2.54	0.0001

Data are represented as mean ± SD.

MDA, CAT, GPx, TAS and TOS levels were significantly different in severe preeclampsia compared with the normal controls. MDA and TOS levels were significantly increased in severe preeclamptic patients compared to control group (Table.3). CAT, GPx and TAS levels were significantly lower in severe preeclamptic pregnants (Table.3). (p<0.05).

4.3. Immunohistochemical Findings

Immunohistochemical staining was performed using the avidin–biotin method to determine the umbilical tissue expressions of Caspase 3. Immunohistochemical examinations demonstrated the presence of Caspase 3 immunostaining in the vascular endothelium. Caspase 3 immunoreactivity was considerably increased in Severe preeclampsia

(S.P) group (p<0.05). Figure 1 show the Caspase 3 expression in S.P group.

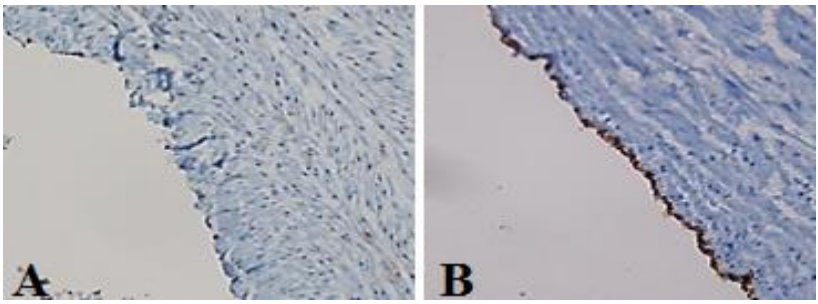

Figure 1. Caspase 3 immunohistochemistry staining. A: Control group, B: Severe Preeclampsia (S.P)

Table 2. Immunoreactivity Intensity Values of Caspase 3 İn The Vessel Endothelium

	Control	S.P	p
Caspase 3	85.02±4.27	107.14±2.19	0.0001

The data are expressed as mean + standart deviation. p<0.05 was accepted as significant.

4.4. Western Blot Findings

β actin was used as a loading control in western blot analysis. According to the results of western blot, a statistically significant increase in the Caspase 3 expression band was found in S.P group (p<0.05). Figure 2 shows the Caspase 3 expression.

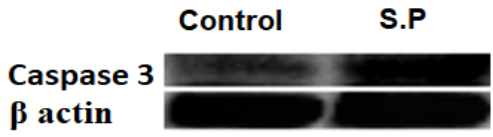

Figure 2: Caspase 3 protein band view

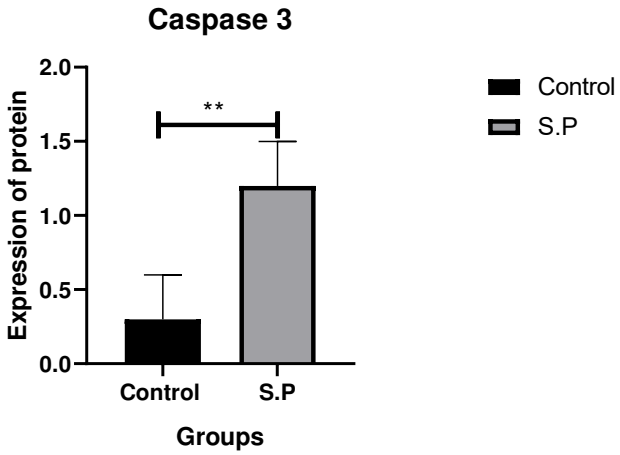

Figure 3: Caspase 3 expression of protein. Abbreviation: S.P, severe preeclampsia.

In addition, the western blot analyses indicated that the protein expression of Caspase 3 was higher in the umbilical tissues of the S.P group than in the control group (Figure 3), (p<0.05).

5. DISSUCION

Preeclampsia is one of the leading reasons of maternal and perinatal mortality and morbidity worldwide (Filipek A, 2018; Rana S, 2019). Although the etiology is not completely understood, the inadequacy of trophoblast infestation and changes in the spiral arteries in the placental bed causes insufficient perfusion of the placenta and thus hypoxia. In other words, preeclampsia is associated with weakened or impaired trophoblast infestation. Spiral artery differentiation and trophoblast proliferation have been reported in patients with preeclampsia (Wright D, 2020; Ives CW, 2020). Decreased uteroplacental perfusion is largely related to endothelial dysfunction in preeclampsia (Sibai B, 2005).

Du L et al. reported that there was no significant difference between preeclampsia and healthy pregnant women in age (Du L, 2017). Similarly, Rath g et al. reported that there was no significant difference in age and height between preeclampsia pregnant women and healthy pregnant women (Rath G, 2016; Adu-Gyamfi EA, 2019). When we look at the age ratio of the groups included in the study; There was no significant difference between severe preeclampsia pregnant women and healthy control group. In the results we found, it was seen that the systolic and diastolic blood pressures of severe preeclamptic pregnant women were significantly higher than the normal pregnant women. In addition, we found uric acid and urine protein of severe preeclamptic pregnant women were significantly higher than the normal pregnant women. These results were similar to previous studies(Du L, 2017; Godhamgaonkar AA, 2021)

There is increasing evidence that oxidative stress in uteroplacental tissues plays a important role in the development of preeclampsia (Jauniaux, E, 2006). Free radicals lead to oxidative damage of cellular macromolecules such as nucleic acids, proteins and lipids in tissues. Increased serum MDA concentrations in preeclamptic women have been shown in previous studies (Fenzl V, 2013; Rafeeinia A, 2014). In a study evaluating GPx, an antioxidant enzyme, the level of GPx was significantly lower in patients with preeclampsia than in the control group (Chamy VM, 2006; Suhail M, 2008). In our study, GPx levels were significantly lower in the preeclampsia group than in the control group. However, tissue MDA was significantly higher in the severe preeclampsia group than in the control group. Some studies have

reported a decrease in CAT level in the preeclampsia group (Yan JY, 2012). In another study, CAT level was higher in the preeclampsia group than in the control group and it was suggested that this elevation might be caused by an adaptive response to compensate for increased oxidative stress (Gohil JT, 2011). In our study, CAT activity was significantly lower in the severe preeclampsia group than in the control group.

The capacity of antioxidants to prevent oxidative damage may play a crucial role in preeclampsia. For this purpose we evaluated TAS and TOS levels in umbilical tissues. Some studies have reported that the level of TAS in placentas of severe preeclampsia group is lower than healthy pregnant women (Ozturk E, 2011). Similarly, In our study, we found that TAS levels were lower and TOS levels were higher in umbilical cords of severe preeclampsia pregnant women due to increased oxidative stress.

The apoptosis rate is thought to have increased in preeclampsia as a result of hypoxia reperfusion injury and oxidative stress (Hung T.H, 2012). There are proofs about the enhanced apoptosis in extravillous trophoblasts of placentas from intrauterine growth restriction and preeclampsia pregnancies (Whitley G.S, 2007). The role of exaggerated apoptosis in placental pathology in preeclampsia is not clear, but it may prevent supply of syncytiotrophoblast, support syncytial degeneration and release inflammatory mediators into the maternal circulation (Sharp A.N, 2010). Similar to the previous results, In our study, it was observed that there was a significant

increase in caspase 3 ratio in the umbilical tissues of serious preeclamptic pregnant women compared to normal pregnant women.

Upregulation of MDA, TOS and downregulation of CAT, GPx and TAS were consistent with apoptosis in the severe preeclampsia umbilical cords. These results may contribute to the pathophysiology of severe preeclampsia.

REFERENCES

Abad C, Proverbio T, Piñero S, Botana D, Chiarello DI, Marín R, Proverbio F. (2012). Preeclampsia, placenta, oxidative stress, and PMCA. Hypertens Pregnancy. Vol.31, No.4, pp:427-441.

Adu-Gyamfi EA, Fondjo LA, Owiredu WKBA, Czika A, Nelson W, Lamptey J, Wang YX, Ding YB. (2019). The role of adiponectin in placentation and preeclampsia. Cell Biochem Funct. Vol. 38, No. 1, (Jan, 2020), pp: 106-117.

Ahmad IM, Zimmerman MC, Moore TA. (2019). Oxidative stress in early pregnancy and the risk of preeclampsia. Pregnancy Hypertens. Vol.18, (Oct, 2019), pp: 99-102.

Chamy VM, Lepe J, Catalan A, Retamal D, Escobar JA, Madrid EM. (2006). Oxidative stress is closely related to clinical severity of preeclampsia. Biol Res. 2006, Vol. 39, No. 2, (2006), pp: 229-236.

Du L, He F, Kuang L, Tang W, Li Y, Chen D. (2017). eNOS/iNOS and endoplasmic reticulum stress-induced apoptosis in the placentas of patients with preeclampsia. J Hum Hypertens. Vol. 31, No. 1, (Jan, 2017), pp: 49-55.

Duley L. (2009). The global impact of pre-eclampsia and eclampsia, Semin Perinatol. Vol.33, No. 3, (Jun, 2009), pp: 130–137.

Elliot MG. (2016). Oxidative stress and the evolutionary origins of preeclampsia. J Reprod Immunol. Vol. 114, (Apr, 2016), pp: 75-80.

Fenzl V, Flegar-Meštrić Z, Perkov S, Andrišić L, Tatzber F, Žarković N, Duic Z. (2013). Trace elements and oxidative stress in hypertensive disorders of pregnancy. Arch Gynecol Obstet, Vol. 287, No. 1, (Jan, 2013), pp: 19–24

Filipek A, Jurewicz E. (2018). Preeclampsia - a disease of pregnant women. Postepy Biochem, Vol. 64, No. 4, (Dec, 2018), pp:232-229.

Godhamgaonkar AA, Sundrani DP, Joshi SR. (2021). Role of maternal nutrition and oxidative stress in placental telomere attrition in women with preeclampsia. Hypertens Pregnancy. Vol. 40, No. 1, (Feb, 2021), pp: 63-74.

Gohil JT, Patel PK, Gupta P. (2011). Evaluation of oxidative stress and antioxidant defence in subjects of preeclampsia. J Obstet Gynaecol India, Vol. 61, No. 6, (Dec, 2011), pp: 638-640.

Gupta S, Agarwal A, Sharma RK. (2005). The role of placental oxidative stress and lipid peroxidation in preeclampsia. Obstet Gynecol Surv. Vol. 60, No. 12, (Dec, 2005), pp:807-816.

Gupta S, Aziz N, Sekhon L, Agarwal R, Mansour G, Li J, Agarwal A. (2009). Lipid peroxidation and antioxidant status in preeclampsia: a systematic review, Obstet Gynecol Surv, Vol. 64, No. 11, (Nov, 2009), pp: 750-759.

Hsieh TT, Chen SF, Lo LM, Li MJ, Yeh YL, Hung TH. (2012). The Association Between Maternal Oxidative Stress at Mid-Gestation and Subsequent Pregnancy Complications Reproductive Sciences, Vol. 19, No. 5, (May, 2012), pp: 505-512.

Hung, T.H, Chen, S.F, Lo, L.M, Li, M.J, Yeh, Y.L, Hsieh, T.T. (2012). Increased autophagyin placentas of intrauterine growth-restricted pregnancies. PLoS ONE, Vol. 7, No. 7, e40957.

Ishihara, N, Matsuo, H, Murakoshi, H, Laoag-Fernandez, J.B, Samoto, T, Maruo, T. (2002). Increased apoptosis in the syncytiotrophoblast in human term placentascomplicated by either preeclampsia or intrauterine growth retardation. Am. J.Obstet. Gynecol, Vol. 186, No. 1, (Jan, 2002), pp: 158–166.

Ives CW, Sinkey R, Rajapreyar I, Tita ATN, Oparil S. (2020). Preeclampsia-Pathophysiology and Clinical Presentations: JACC State-of-the-Art Review. J Am Coll Cardiol. Vol. 76, No. 14, (Oct, 2020), pp: 1690-1702.

Jauniaux, E, Poston, L, Burton, G.J, 2006. Placental-related diseases of pregnancy: involvement of oxidative stress and implications in human evolution. Hum. Reprod, Vol. 12, No. 6, (Nov-Dec, 2006), pp: 747-755.

Lisonkova S, Sabr Y, Mayer C, Young C, Skoll A, Joseph KS. (2014). Maternal morbidity associated with early-onset and late-onset preeclampsia, Obstet Gynecol, Vol. 124, No. 4, (Oct, 2014), pp: 771-781.

Martinvalet D, Zhu P and Lieberman J. (2005). Granzyme A induces caspase-independent mitochondrial damage, a required first step for apoptosis. Immunity, Vol. 22, No. 3, (Mar, 2005), pp: 355-370

Ozturk E, Balat O, Acılmıs YG, Ozcan C, Pence S, Erel Ö. (2011). Measurement of the placental total antioxidant status in preeclamptic women using a novel automated method. J. Obstet. Gynaecol. Res, Vol. 37, No. 4, (Apr, 2011), pp: 337-342.

Öztürk E, Kaymak E, Akin AT, Karabulut D, Ünsal HM, Yakan B. (2020). Thymoquinone is a protective agent that reduces the negative effects of doxorubicin in rat testis. Hum Exp Toxicol, Vol, 39, No. 10, (Oct, 2020), pp: 1364-1373.

Rafeeinia A, Tabandeh A, Khajeniazi S, Marjani AJ. (2014). Serum copper, zinc and lipid peroxidation in pregnant women with preeclampsia in gorgan. Open Biochem J, Vol. 1, No. 8, (Nov, 2014), pp: 83-88.

Rana S, Lemoine E, Granger JP, Karumanchi SA. (2019). Preeclampsia: Pathophysiology, Challenges, and Perspectives. Circ Res, Vol. 124, No. 7, (Mar, 2019), pp: 1094-1112.

Rath G, Aggarwal R, Jawanjal P, Tripathi R, Batra A. (2016). HIF-1 Alpha and Placental Growth Factor in Pregnancies Complicated With Preeclampsia: A Qualitative and Quantitative Analysis. J Clin Lab Anal, Vol. 30, No. 1, (Jan, 2016), pp: 75-83.

Sharp, A.N, Heazell, A.E., Crocker, I., Mor, G. (2010). Placental apoptosis in health and disease. Am. J. Reprod. Immunol, Vol. 64, No. 3, (Sep, 2010), pp: 159–169.

Sibai B, Dekker G, Kupferminc M. (2005). Pre-eclampsia. Lancet, Vol. 365, No. 9461, (Feb, 2005), pp: 785-799

Suhail M, Suhail MF, Khan H. (2008). Role of vitamin C and E in regulating antioxidant and prooxidant markers in preeclampsia. J Clin Biochem Nutr, Vol. 43, No. 3, (Nov, 2008), pp: 210-220.

Whitley, G.S, Dash, P.R., Ayling, L.J., Prefumo, F., Thilaganathan, B., Cartwright,J.E. (2007). Increased apoptosis in first trimester extravillous

trophoblasts frompregnancies at higher risk of developing preeclampsia. Am. J. Pathol, Vol. 170, No. 6, (Jun, 2007), pp: 1903-1909.

Wright D, Wright A, Nicolaides KH. (2020). The competing risk approach for prediction of preeclampsia. Am J Obstet Gynecol, Vol. 223, No. 1, (Jul, 2020), pp: 12-23.

Yan JY, Xu X. (2012). Relationships between concentrations of free fatty acid in serum and oxidativedamage levels in placental mitochondria and preeclampsia. Zhonghua Fu Chan Ke Za Zhi, Vol. 47, No. 6, (Jun, 2012), pp: 412-417.

CHAPTER 6

IMAGING METHODS IN NEUROSURGERY

Assist. Prof. Dr. Bülent ÖZDEMİR[1]

[1]Recep Tayyip Erdogan University Medical Faculty, Department of Neurosurgery, Rize, Turkey .e-mail: bulent.ozdemir@erdogan.edu.tr .
ORCID ID 0000-0002-7635-9808

INTRODUCTION

Neurosurgery is a discipline involving complex interventions due to the complex anatomical structure of the brain. Modern neurosurgery aims to improve survival rates and quality of life in patients with intracranial lesions that are treatable. As in all fields of medicine, advancements in the field of radiology and imaging techniques had led to an evolution in neurosurgery. Imaging modalities have a critical importance for neurosurgery due to various reasons. The object of surgery is often difficult to access, because it is probably within the cranium and surrounded by critical tissues that are vulnerable to manipulation (Chen 2015). Detection of the region of interest (ROI) as precisely as possible provides reduction in the amount of bones to be removed and minimization of damage to the cortex or vascular system. Whole target tissues can be treated with the aid of neuroimaging. In addition, using neuroimaging methods real-time updates and effectiveness of the procedure can also be monitored.

Imaging-guided neurosurgery (IGN) is defined as the integration of imaging modalities to the planning, execution and postoperative evaluation phases of the surgery (Miner 2017). IGN can be used in biopsies, tumor resection procedures, epileptic foci resection and the treatment of vascular conditions. The use of intraoperative neuroimaging provides resection of the lesion completely with minimum impact on the surrounding healthy tissue, leading to improved operational success and patients outcomes.

This chapter begins with a brief history of neuroimaging and continues with description of imaging modalities commonly used in neurosurgery. In addition, some examples of neuroimaging applications are also presented.

1. HISTORY

Imaging of the brain functions has attracted the interest of scientists for more than two centuries. Scientists have proposed the first popular method in the early years of the 19th century. It was thought that the amount of tissue assigned to a certain cognitive function determines the effect of this function on behaviour (Goyder 1857). It is generally accepted that neuroimaging was introduced in the early 1900s with a technique known as pneumoencephalography. This technique is based on drainage of cerebrospinal fluid from around the brain, which leads to a change in the relative density of the brain, allowing surgeons to obtain better X-ray images. However, this technique has been considered quite unsafe for patients (Beaumont and Graham 1983).

With the end of the 20th century, development of new imaging modalities for localization of neurologic functions had resulted in crucial advancements. Owing to these novel non-invasive or minimally invasive techniques, it has been possible to study neurologic functions in both healthy individuals and those affected by disease or injury. The first forms of magnetic resonance imaging and computed tomography were developed in the 1970s and 1980s. These technologies were significantly less harmful. Later, positron emission tomography (PET) and single photon emission computed tomography

(SPECT) methods have been developed. These methods can produce more than static images of the cerebral structure and therefore enable mapping of brain functions in more detail and dynamically. Finally, utilizing the experience gained from PET and SPECT, functional MRI (fMRI), which paves the way for direct observation of cognitive activities has been developed.

2. IMAGING METHODS USED IN NEUROSURGERY

The most commonly used imaging modalities in neurosurgery include CT, PET, SPECT, MRI, fMRI, Ultrasonography (US), fluoroscopy and optics methods. Each of these techniques has different degrees of invasiveness, spatial and temporal resolution. Spatial resolution is defined as the accuracy of localization of the measured activity within the brain, while temporal resolution refers to how closely the measured activity corresponds to the timing of the actual neural activity.

2.1. Computed tomography (CT)

CT is an imaging modality that uses different projections of the object of interest in order to produce cross-sectional 2D and temporal 3D images. The first Godfrey Hounsfield in 1968. The introduction of CT scanners to clinical practice has been a diagnostic and technological revolution (Curry et al. 1990). A typical examination lasted approximately 25 minutes and processing an image took 7 minutes with this first scanner (Curry et al. 1990). The results can be obtained only after a long-duration analysis process with this scanner. Today, thanks to technological advancements, digital data can be calculated in

a fast way and real-time images can be acquired. Available CT scanners can obtain 0.3-1 mm spatial resolution and less than 1-second temporal resolution (Mahesh 2009). As scanning speeds of CT have increased, its clinical use has become dramatically widespread.

CT is a method preferred for interventional procedures that require cross-sectional imaging such as biopsy (Kolokythas et al. 2009; Gupta et al. 2014). Such procedures involve planning, insertion of a needle/probe, guidance and sampling the lesion (Zausinger et al. 2014).

Intraoperative CT has been used with a great success in spinal surgeries since the beginning of the 2000s. The development of multidetector CT has improved the resolution of soft tissue imaging, and its use in neurosurgery is gradually increasing. The most common usage area of intraoperative CT is spinal surgery and functional neurosurgery.

2.2. Positron emission tomography (PET)

PET is a powerful imaging method that provides visualization of the brain functions. It enables non-invasive quantification of cerebral blood flow, metabolism and receptor binding. Previously, PET has been used rather in study setting because of its relatively high costs and complexity of the supportive infrastructure. In the next years, with the technological developments PET has been introduced in the understanding of disease pathogenesis, helping the diagnosis, and monitoring disease progression and response to treatment (Tai and Piccini 2004).

In PET, a radioactive tracer is introduced to the body through intravenous injection. The tracer is essentially a biological compound labeled with a positron emitting isotope. These isotopes have a short half-life and provide tracers to achieve a balance within the body without prolonged exposure to radiation. The most commonly used tracer is ^{18}F-FDG (Wong et al. 2014). Unlike MRI and CT that provide images of organ anatomy, PET provides these images before disease manifestations appear on CT and MRI images (Kumar et al. 2005). Basic steps of PET imagings include:

- 4-hour fasting
- Fluorodeoxyglucose (FDG) administration as intravenous injection
- Resting of patients with open eyes after injection for 40 minutes
- Imaging does not start earlier than 40 minutes following injection

PET and CT are typically combined in one system. CT provides anatomical referencing, while PET images show tumor activity. PET images are useful in the determination of tumor margins for treatment planning, but they have no soft tissue spatial resolution (Parsai et al. 2009). Tumor margins determined by PET depends on metabolic activity of cancer (Ford et al. 2009).

2.3. Single-photon emission computed tomography (SPECT)

SPECT brain perfusion is a useful imaging modality used to determine the regional distribution of brain perfusion and detect various

abnormalities in the brain using lipophilic radiopharmaceuticals that cross the blood-brain barrier and localize in normal brain tissue (Camargo 2001). In the SPECT imaging of the brain, isotopes that bind to neuro-specific pharmaceuticals in order to evaluate regional cerebral blood flow and indirectly metabolic activity (Holmann and Devous 1992). In early SPECT applications, single-head cameras that produce low-resolution images especially in the deep areas of the brain have been used. However, with the development of multiple-head complex gamma detectors, high-resolution cameras have been introduced with a significantly lower cost compared to PET (George 1991). High-resolution SPECT or hybrid SPECT/CT imaging has been increasingly used in neurosurgery.

Especially when combined with CT, SPECT can highlight mechanical stress and degeneration sites. Postoperative SPECT imaging in neurosurgery is limited with an early period, because osteoblastic activity increased with bone fusion results in high degree of radiotracer uptake. Therefore, SPECT imaging is more helpful in the preoperative period. Precise identification of active degeneration sites with SPECT/CT can eliminate the need for repeated imaging or facet injection, enabling targeted surgical intervention with appropriate clinical findings (Brusko et al. 2019). Advanced contrast resolution of SPECT is the main cause making it superior over the other imaging modalities. If the other imaging methods fail, SPECT can be useful especially when combined with CT (Matar et al. 2013).

SPECT has been widely studied as an aid for establishing the diagnosis of degenerative spine disease, neoplasm in the spine, facetogenic pain and infections (Lehman et al. 2013). In addition, it has been used as a postoperative tool in other medical fields including epilepsy, endocrine and musculoskeletal disorders (Gross et al. 2018).

2.4. Magnetic resonance imaging (MRI)

MRI is based on the magnetic resonance phenomenon and has been used in medical diagnostics since 1977 (Bergese and Puente 2009). With the development of nover and more open scanners, MRI has been used in craniotomies since the mid-1990s (Wirtz et al. 1997). MRI provides close to real-time imaging guidance intraoperatively and it is more accurate than the other navigation tools. When microscopic visualization is proven to be insufficient, MRI is used in the evaluation of dynamic changes in the lesion and surroundings. MRI provides high-resolution soft tissue imaging, spectroscopy and diffusion-weighted imaging that can be used in all stages of neurosurgery (Solomon and Silverman 2010; Devic 2012). Soft tissue and contrast provided by MRI are superior over the other modalities and allows improved tumor localization and margin definition, but durations may be long. In addition, powerful magnetic fields in MRI can affect electronic systems and exert gravitational force on implanted mechanical objects in patients (Jolesz et al. 2014).

In a study by Black et al. on intraoperative MRI; this technique has been successfully used in stereotactic biopsies of intracranial lesions, craniotomy for the excision of intracranial space occupying lesions,

excision of arteriovenous excision, intracranial cyst drainage, cervical spine surgery and interstitial hyperthermia in tumor ablation (Black et al. 1997). In MRI, teamwork, good communication and pre-procedural planning are crucial for good outcome and success.

2.5. Functional magnetic resonance imaging (fMRI)

fMRI is an imaging method based on behaviours of biological tissues under the effect of magnetic fields and also on the measurement of blood oxygenation. fMRI is increasingly being used in the examination of patients at the preoperative stage to evaluate the relationship between functionally eloquent cortex and brain pathology. fMRI has undergone a rapid evolution since its first human application (Belliveau et al. 1991). Recent advancements in the clinical use of fMRI has made acquisition, imaging processing and even integration of the findings for neuro-navigational purposes. Using a static field ranging between 0.5-3 T, fMRI is based on nuclear magnetic resonance (NMR) phenomenon.

Blood oxygenation level dependent (BOLD) fMRI is the most commonly used MRI neuroimaging technique. BOLD fMRI uses the advantage of a tight connection between neuronal activity and blood flow (Ogava et al. 1990). Different hemoglobin sensitivities in different oxygen states explain the mechanism underlying BOLD used in fMRI (Thulborn 2012).

fMRI is better applied especially in cognitive neuroscience rather than clinical practice. For example, it has provided a significant contribution to our insight into memory, cerebral plasticity, resting

state networks and social behaviours (Rosen and Savoy 2012). In clinical settings, although fMRI has been most commonly used in the planning of neurosurgery procedures, it has not been widely adopted. fMRI technique has several limitations. These include imaging statistics (false positive and false negative), head motion, experimental design, structural alterations in the brain, reliability and validity of paradigms, field power, psychological noise, neurovascular matching phenomenon, spatial and temporal resolution (Seixas and Lima 2011).

2.6. Intraoperative ultrasonografi (IoUS)

IoUS is an imaging modality providing useful real-time intraoperative information about location and size/bleeding of tumor, residual tumor/bleeding etc. during cranial surgeries. IoUS uses 0.5-4 MHz frequencies for visualization of internal soft tissue and structure and the images obtained can be merged with the images obtained from the other imaging modalities (Bushberg et al. 2012). IoUS effectively detects deep or superficial cerebral and spinal cord lesions. Studies have shown that IoUS is an effective and reliable method especially when used with a contrast medium, leading this method to gain popularity in neurosurgery (Prada et al. 2015; Prada et al. 2014).

IoUS has significant consequences on the outcomes of both adult and pediatric patients. IoUS is helpful in the localization and precise excision of the pathological lesions during the intraoperative period of neurosurgeries. It helps prediction of surgical pathway in the precise excision of the pathological lesions, while at the same time it enables localization and real-time visualization of residual tumor mass. Even

after brain shift and deformation occur, IoUS is useful when accuracy of conventional navigation systems such as CT and MRI is lost (Prada et al. 2015; Prada et al. 2014). IoUS is easy to use in monitoring progression and/or planning of tumor excision (Mair et al. 2013).

In addition IoUS is also helpful in the differentiation of several ipsilateral pathologies that require neurosurgery such as intracerebral hematoma or subdural hematoma plus brain swelling. IoUS is relatively more cost effective compared to the other imaging modalities. However it has some limitations including effectiveness of the surgeon and long learning curve.

2.7. Fluoroscopy

Fluoroscopy is an imaging method, which uses a rapid repetition rate of X-ray images, providing a close to real-time visualization. Using fluoroscopy, images are acquired with 48 kW and 6 mA.

However, fluoroscopy provides only two dimensional images, and personnel who perform the procedure are exposed to radiation. Fluoroscopy is useful especially when surgical equipment is navigated intraoperatively (Nimski and Carl 2015).

2.8. Optic Methods

The use of optic tools and principles in neurosurgery bates back to the early of 20th century. First, Mooney et al. used fluorescence sodium as a biomarker in intraoperative determination of gliomas (Mooney et al. 2014). Although optic fluorescence methods can be used with open surgical procedures, they are still not approved worldwide (Chen

2015). In some situations, the surgeon obtains fluorescence images or images overlaid the anatomical images from CT or MRI (Sakuma 2014).

Bioluminescence and fluorescence are commonly used optic methods. The most well-known application of fluorescence imaging is surgical guidance during the resection of brain tumors. The most commonly used fluorescence agents are indocyanine green and 4-ALA. These agents can be injected into tumor tissue and highlight the pathology. Since light is easily scattered, reflected and emitted by the tissues, the imaging is confined to 5-8 mm under the surface (Sakuma 2014). Using fluorescence molecules, studies have investigated cellular anatomical structures, neuronal circuit, molecular interactions, cerebral dynamics and pathology (Tung et al. 2016). As an important advantage, fluorescence molecules are much more bright than bioluminescence molecules. However, various specific characteristics make bioluminescence an attractive imaging model. Bioluminescence molecules usually create a higher signal/imaging rate. Therefore, they can be more sensitive compared to fluorescence signals. In addition, bioluminescence does not require exogenous stimulation of light sources, it is more suitable to visualize light sensitive cells such as retinal neurons.

NEUROIMAGING APPLICATIONS IN NEUROSURGERY

Imaging modalities are used alone or in combination for different purposes in neurosurgery. Imaging during surgery improves success of the procedures and patient outcomes by excision of the tumor

thoroughly and accurately, while minimizing damage to surrounding health tissues. Some examples of neuroimaging applications in neurosurgery are given below.

2.9. Biopsies

CT, MRI, fMRI, PET, PET/CT and SPECT are helpful in the evaluation of the presence of tumor, although biopsy is still considered as the gıold standard in malignant/benign differentiation of a mass. Advanced anatomical and molecular imaging modalities can be used in the diagnosis of a lesion, but histological diagnosis required for treatment can be established only with biopsy examination. Serial biopsies can also determine size and histological profile of the lesion and properties of the surrounding tissues.

US guidance for brain biopsy is simple, fast and cost effective. An important advantage of US during biopsy is enabling the surgeon to real-time obtain visual information about brain lesion, shift of the tumor position or post-biopsy complications. However, its resolution is lower than CT and its suitable only for lesions >5mm (Jain et al. 2006).

2.10. Tumor resection

The resection of brain tumors is one of the most complex and precise procedures because of the complex anatomical structure of the brain. An important indicator of success in such procedures is the extent of tumor resection. Using imaging modalities, neurosurgery has

improved the extent of resection and patient outcomes by the detection of residual tumor mass and sparing critical tissues (Chen 2015).

X-ray and CT scans are initially used for diagnostic purposes in brain tumors. However, MRI is generally more useful, because it provides detailed information on cellular structure, tumor type, vascular supply, anatomy, position and size of the tumor, and therefore MRI is the study of choice in brain tumors. Furthermore, fMRI is used in the mapping of brain activity.

2.11. Epilepsy

Despite medical treatment, some epileptic patients require surgical treatment for removal of epileptogenic foci. The role of neuroimaging is the detection of the epileptogenic focus and providing guidance for surgical resection of the focus. CT, MRI, fMRI and electroencephalography (EEG) should be used in combination in order to obtain optimal outcomes in these procedures (Assad and Cosgrove 2015). The diagnosis of epilepsy can be made with aid of SPECT, MRI, CT and PET. Ictal SPECT can be used in localization of the epileptogenic focus, but seizures should be present when the tracer is injected. CT and MRI help localization of epileptogenic foci as well as exclusion of vascular or inflammatory abnormalities. High-resolution MRI is widely used in the detection of the epileptogenic focus preoperatively.

CONCLUSION

Imaging modalities contribute to perform complex neurosurgery procedures more effectively and successfully, and to improve patient outcomes. Today, in parallel with the developments in the fields of digital technologies, telemedicine, robotic surgery etc. imaging methods are being developed continuously and novel techniques are introduced. Thanks to imaging modalities, the evolution of neurosurgery is continuing and it is estimated that this evolution will further accelerate in the near future.

REFERENCES

Asaad, W., & Cosgrove, G. (2015). Imaging and epilepsy: the key to surgical success. In A. J. Golby (Ed.), Image-guided Neurosurgery (pp. 263–276). New York, NY: Elsevier.

Ashraf, M., Choudhary, N., Hussain, S. S., Kamboh, U. A., & Ashraf, N. (2020). Role of intraoperative computed tomography scanner in modern neurosurgery - An early experience. Surgical neurology international, 11, 247.

Beaumont, J. Graham. Introduction to Neuropsychology. New York: The Guilford Press, 1983. 314 pages.

Belliveau, J. W., Kennedy, D. N., Jr, McKinstry, R. C., Buchbinder, B. R., Weisskoff, R. M., Cohen, M. S., Vevea, J. M., Brady, T. J., & Rosen, B. R. (1991). Functional mapping of the human visual cortex by magnetic resonance imaging. Science (New York, N.Y.), 254(5032), 716–719.

Bergese, S. D., & Puente, E. G. (2009). Anesthesia in the intraoperative MRI environment. Neurosurgery clinics of North America, 20(2), 155–162.

Black, P. M., Moriarty, T., Alexander, E., 3rd, Stieg, P., Woodard, E. J., Gleason, P. L., Martin, C. H., Kikinis, R., Schwartz, R. B., & Jolesz, F. A. (1997). Development and implementation of intraoperative magnetic resonance imaging and its neurosurgical applications. Neurosurgery, 41(4), 831–845.

Brusko, G. D., Perez-Roman, R. J., Tapamo, H., Burks, S. S., Serafini, A. N., & Wang, M. Y. (2019). Preoperative SPECT imaging as a tool for surgical planning in patients with axial neck and back pain. Neurosurgical focus, 47(6), E19.

Bushberg, J., Seibert, J., Leidholdt, E., & Boone, J. (2012). The essential physics of medical imaging, (3rd ed.). (pp. 500–575) Philadelphia, PA: Lippincott Williams & Wilkins.

Camargo E. E. (2001). Brain SPECT in neurology and psychiatry. Journal of nuclear medicine : official publication, Society of Nuclear Medicine, 42(4), 611–623.

Chen, X. (2015). Multimodal image-guided brain tumour resection. In A. J. Golby (Ed.), Image-guided Neurosurgery (pp. 213–244). New York, NY: Elsevier

Curry T.S., Dowdey J., Murry R. Christensen's physics of diagnostic radiology. Lea & Febiger, Philadelphia 1990.

Devic, S. (2012). MRI simulation for radiotherapy treatment planning. Med Phys 39(11), 6701–6711.

Ford, E., Herman, J., Yorke, E., & Wahl, L. (2009). 18F-FDG PET/ CT for image-guided and intensity-modulated radiotherapy. J Nucl Med 50, 655–1665.

George, MS. Neuroactivation and Neuroimaging with SPET. New York, NY, SpringerVerlag, 1991

Gross, C. E., Barfield, W., Schweizer, C., Rasch, H., Hirschmann, M. T., Hintermann, B., & Knupp, M. (2018). The utility of the ankle SPECT/CT scan to predict functional and clinical outcomes in supramalleolar osteotomy patients. Journal of orthopaedic research : official publication of the Orthopaedic Research Society, 36(7), 2015–2021.

Goyder DG. My Battle for Life: The Autobiography of a Phrenologist. London, United Kingdom; Simpkin, Marshall, and Co; 1857.

Gupta, R., Walsh, C., Wang, I., Kachelrieb, M., Kuntz, & Bartling, S. (2014). CT-guided interventions: current practice and future directions. In F. Jolesz (Ed.), Intraoperative Imaging and Image-guided Therapy (pp. 173–192). New York, NY: Springer.

Holman, B. L., & Devous, M. D., Sr (1992). Functional brain SPECT: the emergence of a powerful clinical method. Journal of nuclear medicine : official publication, Society of Nuclear Medicine, 33(10), 1888–1904.

Jain, D., Sharma, M. C., Sarkar, C., Gupta, D., Singh, M., & Mahapatra, A. K. (2006). Comparative analysis of diagnostic accuracy of different brain biopsy procedures. Neurology India, 54(4), 394–398.

Jolesz, F., Golby, A., & Orringer, D. (2014). Magnetic resonance image-guided neurosurgery. In F. Jolesz (Ed.), Intraoperative Imaging and Image-guided Therapy (pp. 451–463). New York, NY: Springer Heidelberg.

Kolokythas, O., Shibata, D., & Dubinsky, T. (2009). Medical imaging. In S. Vaezy & V. Zderic (Eds.), Image-guided Therapy Systems (pp. 18– 53). Norwood, MA: Artech House.

Kumar, S., Rajshekher, G., & Prabhakar, S. (2005). Positron emission tomography in neurological diseases. Neurology India, 53(2), 149–155.

Lehman, V. T., Murphy, R. C., & Maus, T. P. (2013). 99mTc-MDP SPECT/CT of the spine and sacrum at a multispecialty institution: clinical use, findings, and impact on patient management. Nuclear medicine communications, 34(11), 1097–1106.

Mahesh, M. (2009). ‘‘MDCT Physics. The Basics’’. Philadelphia, PA: Lippincott Williams & Wilkins.

Mair, R., Heald, J., Poeata, I., & Ivanov, M. (2013). A practical grading system of ultrasonographic visibility for intracerebral lesions. Acta neurochirurgica, 155(12), 2293–2298.

Matar, H. E., Navalkissoor, S., Berovic, M., Shetty, R., Garlick, N., Casey, A. T., & Quigley, A. M. (2013). Is hybrid imaging (SPECT/CT) a useful adjunct in the management of suspected facet joints arthropathy?. International orthopaedics, 37(5), 865–870.

Miner R. C. (2017). Image-Guided Neurosurgery. Journal of medical imaging and radiation sciences, 48(4), 328–335.

Mooney, M. A., Zehri, A. H., Georges, J. F., & Nakaji, P. (2014). Laser scanning confocal endomicroscopy in the neurosurgical operating room: a review and discussion of future applications. Neurosurgical focus, 36(2), E9.

Nimsky, C., & Carl, B. (2015). Intraoperative imaging. In A. J. Golby (Ed.), Image-guided Neurosurgery (pp. 163–190). New York, NY: Elsevier.

Ogawa, S., Lee, T. M., Kay, A. R., & Tank, D. W. (1990). Brain magnetic resonance imaging with contrast dependent on blood oxygenation. Proceedings of the National Academy of Sciences of the United States of America, 87(24), 9868–9872.

Parsai, E., Doblelbower, M., & Doblelbower, R. (2009). Image-guided radiation therapy: from concept to practice. In S. Vaezy & V. Zderic (Eds.), Image-guided Therapy Systems (pp. 75–95). Norwood, MA: Artech House.

Prada, F., Del Bene, M., Saini, M., Ferroli, P., & DiMeco, F. (2015). Intraoperative cerebral angiosonography with ultrasound contrast agents: how I do it. Acta neurochirurgica, 157(6), 1025–1029.

Prada, F., Mattei, L., Del Bene, M., Aiani, L., Saini, M., Casali, C., Filippini, A., Legnani, F. G., Perin, A., Saladino, A., Vetrano, I. G., Solbiati, L., Martegani, A., & DiMeco, F. (2014). Intraoperative cerebral glioma characterization with contrast enhanced ultrasound. BioMed research international, 2014, 484261.

Rosen, B. R., & Savoy, R. L. (2012). fMRI at 20: has it changed the world?. NeuroImage, 62(2), 1316–1324.

Sakuma, I. (2014). Optical navigation. In F. Jolesz (Ed.), Intraoperative Imaging and Image-guided Therapy (pp. 581–590). New York, NY: Springer Heidelberg.

Seixas, D., & Lima, D. (2011). Accuracy, reliability, validity and limitations of functional and structural magnetic resonance imaging data. Cortex; a journal devoted to the study of the nervous system and behavior, 47(10), 1266–1269.

Solomon, S., & Silverman, S. (2010). Imaging in interventional oncology. Radiology 257, 624–640.

Tai, Y. F., & Piccini, P. (2004). Applications of positron emission tomography (PET) in neurology. Journal of neurology, neurosurgery, and psychiatry, 75(5), 669–676.

Thulborn K. R. (2012). My starting point: the discovery of an NMR method for measuring blood oxygenation using the transverse relaxation time of blood water. NeuroImage, 62(2), 589–593.

Tung, J. K., Berglund, K., Gutekunst, C. A., Hochgeschwender, U., & Gross, R. E. (2016). Bioluminescence imaging in live cells and animals. Neurophotonics, 3(2), 025001.

Wirtz, C. R., Bonsanto, M. M., Knauth, M., Tronnier, V. M., Albert, F. K., Staubert, A., & Kunze, S. (1997). Intraoperative magnetic resonance imaging to update interactive navigation in neurosurgery: method and preliminary experience. Computer aided surgery : official journal of the International Society for Computer Aided Surgery, 2(3-4), 172–179.

Wong, F., & Hicks, M. (2014). Multimodality image-guided treatment. In X. Chen & S. Wong (Eds.), Cancer Theranostics (pp. 201–225). San Diego, CA: Elsevier.

Zausinger, S., Schichor, C., Uhl, E., Reiser, M., & Tonn, J. (2014). Intraoperative angiography in neurosurgery. In F. Jolesz (Ed.), Intraoperative Imaging and Image-guided Therapy (pp. 537–548). New York, NY: Springer Heidelberg.

ISBN: 978-625-7636-85-8